Table 3 Lethal arrhythmias and mortality in an I/R rat model

	Number	VT/VF duration (sec)	Mortality (%)
Saline	7	195±42	71
Empty liposomes	6	162±31	50
Amiodarone (3 mg/kg)	6	167±78	33
Amiodarone (10 mg/kg)	6	36±12*	0#
Liposomal Amiodarone (3 mg/kg)	6	18±9*	0#

*$p<0.05$ versus saline (VT/VF duration). #$p<0.05$ versus saline group (mortality). *VT* ventricular tachycardia, *VF* ventricular fibrillation

Minimal Negative Hemodynamic Effects of Liposomal Amiodarone

Amiodarone causes hypotension and bradycardia in clinical settings [4, 5]. In this study, both free and liposomal amiodarone significantly reduced the HR and systolic BP; however, the time-course changes for both the HR and systolic BP in the liposomal amiodarone group were significantly smaller compared with those following the corresponding dose of free amiodarone. Importantly, the reductions in HR and systolic BP at 1, but not 3, minutes after liposomal amiodarone administration were significantly smaller compared with those following the corresponding dose of amiodarone. These findings suggest that liposomal amiodarone may minimize the negative effects on systemic hemodynamics immediately after the administration of amiodarone. One possible mechanism to explain this finding is that amiodarone on the surface of the liposome membrane is covered with PEG so that amiodarone cannot act directly on cardiovascular cells. Gradual release of amiodarone from liposome may minimize the rapid hemodynamic changes, because systemic hemodynamic effects of liposomal amiodarone were significantly attenuated in liposomal amiodarone group than free amiodarone group.

Augmented Anti-arrhythmic Effects of Liposomal Amiodarone

In this study, liposomal amiodarone (3 mg/kg), but not the corresponding dose of free amiodarone (3 mg/kg), significantly reduced the VT/VF duration and mortality compared with saline in an I/R rat model. Because the acute effects of amiodarone are known to be attributable to blockade of Na^+, Ca^{2+} and dose-dependent K^+ channels [2, 25], increasing the concentration of amiodarone in the I/R myocardium may augment its anti-arrhythmic effects through its tonic effects on cardiomyocytes caused by blocking cardiac ionic currents. Kishida et al. reported that amiodarone enhances nitric oxide production in cultured human endothelial cells [26]. Furthermore, amiodarone protects cardiac myocytes against oxidative injury by scavenging free radicals [27]. These pleiotropic effects of amiodarone are also enhanced by its increased concentration in the I/R myocardium via PEGylated liposomes, which may contribute to the reduction of lethal arrhythmias during reperfusion followed by ischemia. In the present study, since we did not do any procedure such as electrical conversion or cardiac massage for VT/VF, the mortality was higher than in our previous report [16].

Clinical Implications

In clinical settings, higher doses of amiodarone cause hypotension and non-cardiac death or induce worsening heart failure through negative inotropic effects [28]. These effects often diminish the beneficial effects of amiodarone for patients with AMI or heart failure [8, 9]. The present study demonstrated that liposomal amiodarone (3 mg/kg) exerts anti-arrhythmic effects similar to a high dose of free amiodarone (10 mg/kg) while reducing the extent of bradycardia and hypotension, suggesting that encapsulating amiodarone in liposomes augments its anti-arrhythmic effects and reduces its negative effects on hemodynamic parameters with reducing administrative dose. These findings can have a great impact on preventing lethal arrhythmias during reperfusion in AMI patients.

Study Limitations

There are several limitations in this study. We used a brief period of I/R without myocardial infarction in rats. Sakamoto et al. demonstrated that the incidence of VT/VF in a rodent model was 'bell-shaped' with a maximum at 5 min of ischemia and that most lethal arrhythmias occurred within first 20 s after the onset of reperfusion [29]. Consistently, our data showed that the mean time at which the lethal arrhythmia occurred after the onset of reperfusion was 3.3+/−1.6 s. Therefore, we chose the 5 min of ischemia followed by 15 min of reperfusion model. We also chose the timing of drug administration before the onset of ischemia to clarify whether liposomal-amiodarone could prevent the lethal arrhythmia that occurs in the early period of reperfusion. In addition, in clinical practice lethal arrhythmias often occur after a brief period of I/R without any irreversible damage to the heart, indicating that the anti-arrhythmic effects of liposomal amiodarone during a brief period of ischemia model could have clinical relevance [30]. However, careful interpretation is necessary when using liposomal amiodarone in acute myocardial infarction with irreversible damage to confirm the beneficial effects of liposomal amiodarone. Furthermore, because the electrophysiology of rats differs from that of humans and drug administration in our study started before the onset of

ischemia, additional pre-clinical studies including a longer period of I/R model to consider the timing of drug administration are needed using large animal models. We should also take into account that the potential side effects of amiodarone such as bradycardia are minimal in the left coronary artery occlusion model used in the present study.

Conclusion

In conclusion, the targeted delivery of liposomal amiodarone to the I/R myocardium exerted strong anti-arrhythmic effects and reduced the negative impact on systemic hemodynamics. Nano-sized liposomes may be a promising drug delivery system for targeting the I/R myocardium with cardioprotective agents.

Acknowledgments The authors thank Takaki Hayakawa for her technical assistance, Takeshi Aiba for his special advice about data analysis. This research was supported by Grants-in-Aid from the Ministry of Health, Labor, and Welfare of Japan; Grants-in-Aid from the Ministry of Education, Culture, Sports, Science, and Technology of Japan; grants from the Japan Heart Foundation; and grants from the Japan Cardiovascular Research Foundation.

References

1. Di Diego JM, Antzelevitch C. Ischemic ventricular arrhythmias: experimental models and their clinical relevance. Hear Rhythm. 2011;8:1963–8.
2. Kodama I, Kamiya K, Toyama J. Cellular electropharmacology of amiodarone. Cardiovasc Res. 1997;35:13–29.
3. Vassallo P, Trohman RG. Prescribing amiodarone: an evidence-based review of clinical indications. JAMA. 2007;298:1312–22.
4. Scheinman MM, Levine JH, Cannom DS, et al. Dose-ranging study of intravenous amiodarone in patients life-threatening ventricular tachyarrhythmias. The Intravenous Amiodarone Muticenter Investigators Group. Circulation. 1995;92:3264–72.
5. Podrid PJ. Amiodarone; reevaluation of an old drug. Ann Intern Med. 1995;122:689–700.
6. Shiga T, Tanaka T, Irie S, Hagiwara N, Kasanuki H. Pharmacokinetics of intravenous amiodarone and its electrocardiographic effects on healthy Japanese subjects. Hear Vessel. 2011;26:274–81.
7. Wenzel V, Russo SG, Arntz HR, et al. [Comments on the 2010 guidelines on cardiopulmonary resuscitation of the European Resuscitation Council.]. Anaesthesist. 2010.
8. Elizari MV, Martínez JM, Belziti C, et al. Morbidity and mortality following early administration of amiodarone in acute myocardial infarction. GEMICA study investigators, GEMA Group, Buenos Aires, Argentina. Grupo de Estudios Multicentricos en Argentina. Eur Heart J. 2000;21:198–205.
9. Hu K, Gaudron P, Ertl G. Effects of high- and low-dose amiodarone on mortality, left ventricular remodeling, and hemodynamics in rats with experimental myocardial infarction. J Cardiovasc Pharmacol. 2004;44:627–30.
10. Semalty A, Semalty M, Rawat BS, Singh D, Rawat MS. Pharmacosomes: the lipid-based new drug delivery system. Expert Opin Drug Deliv. 2009;6:599–612.
11. Whitehead KA, Langer R, Anderson DG. Knocking down barriers: advances in siRNA delivery. Nat Rev Drug Discov. 2009;8:129–38.
12. Malam Y, Loizidou M, Seifalian AM. Liposomes and nanoparticles: nanosized vehicles for drug delivery in cancer. Trends Pharmacol Sci. 2009;30:592–9.
13. Horwitz LD, Kaufman D, Keller MW, Kong Y. Time course of coronary endothelial healing after injury due to ischemia and reperfusion. Circulation. 1994;90:2439–47.
14. Dauber IM, VanBenthuysen KM, McMurtry IF, et al. Functional coronary microvascular injury evident as increased permeability due to brief ischemia and reperfusion. Circ Res. 1990;66:986–98.
15. Galagudza MM, Korolev DV, Sonin DL, et al. Targeted drug delivery into reversibly injured myocardium with silica nanoparticles: surface functionalization, natural biodistribution, and acute toxicity. Int J Nanomedicine. 2010;5:231–7.
16. Takahama H, Minamino T, Asanuma H, et al. Prolonged targeting of ischemic/reperfused myocardium by liposomal adenosine augments cardioprotection in rats. J Am Coll Cardiol. 2009;53:709–17.
17. Riva E, Hearse DJ. Anti-arrhythmic effects of amiodarone and desethylamiodarone on malignant ventricular arrhythmias arising as a consequence of ischaemia and reperfusion in the anaesthetised rat. Cardiovasc Res. 1989;23:331–9.
18. Canyon SJ, Dobson GP. Protection against ventricular arrhythmias and cardiac death using adenosine and lidocaine during regional ischemia in the in vivo rat. Am J Physiol Heart Circ Physiol. 2004;287:H1286–95.
19. Plomp TA, Wiersinga WM, Maes RA. Tissue distribution of amiodarone and desethylamiodarone in rats after repeated oral administration of various amiodarone dosages. Arzneimittelforschung. 1985;35:1805–10.
20. Feige JN, Sage D, Wahli W, Desvergne B, Gelman L. PixFRET, an ImageJ plug-in for FRET calculation that can accommodate variations in spectral bleed-trhoughs. Microsc Res Tech. 2005;68:51–8.
21. Opitz CF, Mitchell GF, Pfeffer MA, Pfeffer JM. Arrhythmias and death after coronary artery occlusion in the rat. Continuous telemetric ECG monitoring in conscious, untethered rats. Circulation. 1995;92:253–61.
22. Klibanov AL, Maruyama K, Torchilin VP, Huang L. Amphipathic polyethyleneglycols effectively prolong the circulation time of liposomes. FEBS Lett. 1990;268:235–7.
23. Theodossiou TA, Galanou MC, Paleos CM. Novel amiodarone-doxorubicin cocktail liposomes enhance doxorubicin retention and cytotoxicity in DU145 human prostate carcinoma cells. J Med Chem. 2008;51:6067–74.
24. Elhasi S, Astaneh R, Lavasanifar A. Solubilization of an amphiphilic drug by poly(ethylene oxide)-block-poly(ester) micelles. Eur J Pharm Biopharm. 2007;65:406–13.
25. Kamiya K, Nishiyama A, Yasui K, Hojo M, Sanguinetti MC, Kodama I. Short- and long-term effects of amiodarone on the two components of cardiac delayed rectifier K(+) current. Circulation. 2001;9:1317–24.
26. Kishida S, Nakajima T, Ma J, et al. Amiodarone and N-desethylamiodarone enhance endothelial nitric oxide production in human endothelial cells. Int Heart J. 2006;47:85–93.
27. Ide T, Tsutsui H, Kinugawa S, Utsumi H, Takeshita A. Amiodarone protects cardiac myocytes against oxidative injury by its free radical scavenging action. Circulation. 1999;100:690–2.
28. Freedman MD, Somberg JC. Pharmacology and pharmacokinetics of amiodarone. J Clin Pharamacol. 1991;31:1061–9.
29. Sakamoto J, Miura T, Tsuchida A, Fukuma T, Hasegawa T, Shimamoto K. Reperfusion arrhythmias in the murine heart: their characteristics and alteration after ischemic preconditioning. Basic Res Cardiol. 1999;94:489–95.
30. Tzivoni D, Keren A, Granot H, Gottlieb S, Benhorin J, Stern S. Ventricular fibrillation caused by myocardial reperfusion in Prinzmetal's angina. Am Heart J. 1983;105:323–5.

The FASEB Journal • Research Communication

Treatment of cerebral ischemia-reperfusion injury with PEGylated liposomes encapsulating FK506

Takayuki Ishii,* Tomohiro Asai,* Dai Oyama,* Yurika Agato,* Nodoka Yasuda,* Tatsuya Fukuta,* Kosuke Shimizu,* Tetsuo Minamino,† and Naoto Oku*,[1]

*Department of Medical Biochemistry, School of Pharmaceutical Sciences, University of Shizuoka, Shizuoka, Japan; and †Department of Cardiovascular Medicine, Osaka University Graduate School of Medicine, Osaka, Japan

ABSTRACT **FK506 (Tacrolimus) has the potential to decrease cerebral ischemia-reperfusion injury. However, the clinical trial of FK506 as a neuroprotectant failed due to adverse side effects. This present study aimed to conduct the selective delivery of FK506 to damaged regions, while at the same time reducing the dosage of FK506, by using a liposomal drug delivery system. First, the cytoprotective effect of polyethylene glycol-modified liposomes encapsulating FK506 (FK506-liposomes) on neuron-like pheochromocytoma PC12 cells was examined. FK506-liposomes protected these cells from H_2O_2-induced toxicity in a dose-dependent manner. Next, we investigated the usefulness of FK506-liposomes in transient middle cerebral artery occlusion (t-MCAO) rats. FK506-liposomes accumulated in the brain parenchyma by passing through the disrupted blood-brain barrier at an early stage after reperfusion had been initiated. Histological analysis showed that FK506-liposomes strongly suppressed neutrophil invasion and apoptotic cell death, events that lead to a poor stroke outcome. Corresponding to these results, a single injection of FK506-liposomes at a low dosage significantly reduced cerebral cell death and ameliorated motor function deficits in t-MCAO rats. These results suggest that liposomalization of FK506 could reduce the administration dose by enhancing the therapeutic efficacy; hence, FK506-liposomes should be a promising neuroprotectant after cerebral stroke.—Ishii, T., Asai, T., Oyama, D., Agato, Y., Yasuda, N., Fukuta, T., Shimizu, K., Minamino, T., Oku, N. Treatment of cerebral ischemia-reperfusion injury with PEGylated liposomes encapsulating FK506. *FASEB J.* 27, 1362–1370 (2013). www.fasebj.org**

Key Words: neuroprotectant · tacrolimus · apoptosis · inflammation · motor function

AFTER RESTORATION OF BLOOD FLOW in cerebral stroke patients, cerebral ischemia-reperfusion (I/R) injury often occurs, resulting in neurological deficits (1, 2). Hence, the development of neuroprotective therapy for this type of injury has been awaited for a better outcome after a cerebral stroke. Although >1000 candidate compounds have shown potency as a neuroprotectant, and >100 of them have been tested in clinical studies in the past, none of them have passed these trials due to insufficiency of medicinal efficacy and to adverse side effects (3, 4). To overcome the present situation, we previously applied the liposomal drug delivery system (DDS) to the treatment of cerebral I/R injury (5). When 100 nm liposomes were intravenously injected immediately after the start of reperfusion, they selectively accumulated in the I/R region, suggesting that drug delivery using liposomes is applicable for treatment of I/R injuries. Moreover, liposomes modified with the antiapoptotic protein asialoerythropoietin significantly suppressed cerebral cell death and improved motor functional deficits induced by I/R injury in transient middle cerebral artery occlusion (t-MCAO) rats by increasing the accumulation of the protein in the injured region compared with the outcome for the free asialoerythropoietin-treated group. This finding offers the possibility that liposomal DDS could be a useful strategy for the treatment of cerebral I/R injury. However, the efficacy of liposomal DDS for treatment of cerebral I/R injuries has been proven for just a single protein, *i.e.*, asialoerythropoietin. Accordingly, more study is needed to reinforce the utility of this therapeu-

Abbreviations: DDS, drug delivery system; DiI-C_{18}, 1,1′-dioctadecyl-3,3,3′,3′-tetramethylindocarbocyanine; DPPC, dipalmitoylphosphatidylcholine; DSPE, distearoylphosphatidylethanolamine; FK506-liposome, polyethylene glycol-modified liposomes encapsulating FK506; HCO-60, polyoxyethylene (60) hydrogenated castor oil; HS, horse serum; ICA, internal carotid artery; I/R, ischemia-reperfusion; IVIS, *in vivo* imaging system; MCA, middle cerebral artery; MPO, myeloperoxidase; NGF, nerve growth factor; PEG, polyethylene glycol; t-MCAO, transient middle cerebral artery occlusion; TTC, 2,3,5-triphenyltetrazolium chloride; TTW, therapeutic time window; TUNEL, terminal deoxyribonucleotidyl transferase (TDT)-mediated dUTP-digoxigenin nick end labeling

[1] Correspondence: Department of Medical Biochemistry, School of Pharmaceutical Sciences, University of Shizuoka, 52-1 Yada, Suruga-ku, Shizuoka 422-8526, Japan. E-mail: oku@u-shizuoka-ken.ac.jp

doi: 10.1096/fj.12-221325

This article includes supplemental data. Please visit *http://www.fasebj.org* to obtain this information.

0892-6638/13/0027-1362 © FASEB

tic strategy. The therapeutic effect of liposomes encapsulating a neuroprotective chemodrug on I/R injury has not been examined yet. Therefore, in this study designed for achieving this purpose and developing a novel neuroprotectant, we prepared polyethylene glycol (PEG)-modified liposomes encapsulating FK506 (FK506-liposomes).

The immunosuppressant FK506 has been widely used to prevent allograft rejections in clinical organ transplantation, and was also recently reported to be a drug candidate for the treatment of acute stroke in animal studies (6–8). Calcineurin is activated by excessive influx of Ca^{2+} into cerebral cells after a cerebral ischemic event, resulting in the induction of nitric oxide, generation of inflammatory cytokines, and the release of cytochrome *c* (9–12). FK506 inhibits the activation of calcineurin by associating with the FK506-binding protein (FKBP) in neuronal cells and glial cells; hence, it shows a neuroprotective effect on experimental stroke models. However, the frequent administration of FK506 required to achieve a good outcome has the risk of developing side effects such as heart deficits and nephrotoxicity. The liposomalization of FK506 is a promising approach for changing the biodistribution and negating the problem of poor water solubility (13, 14). The liposomal formulation of FK506 is as effective as an equal dose of commercial FK506 in preventing the rejection of transplant grafts, but with considerably less nephrotoxicity (14). The efficient delivery of FK506 to ischemic regions by using liposomes might potentially reduce the administration dosage without changing neuroprotective efficacy. In the present study, we assessed the potential of FK506-liposomes as a neuroprotectant against cerebral I/R injury by investigating their cerebral distribution, pharmacological activity, therapeutic effect, and therapeutic time window in t-MCAO rats.

MATERIALS AND METHODS

Animals

Male Wistar rats (170–210 g) were purchased from Japan SLC, Inc. (Shizuoka, Japan). The animals were cared for according to the Animal Facility Guidelines of the University of Shizuoka. All animal procedures were approved by the Animal and Ethics Review Committee of the University of Shizuoka.

Preparation of FK506-liposomes

The lipid composition of FK506-liposomes was dipalmitoylphosphatidylcholine (DPPC) and distearoylphosphatidylethanolamine (DSPE)-PEG (molecular weight of PEG was 2000) in a 20:1 molar ratio. FK506-liposomes were prepared by the following freeze-drying method: FK506 was dissolved in methanol and added to a flask containing the above lipids dissolved in *tert*-butylalcohol. The molar ratio of FK506 to DPPC was 1:50. The solution was lyophilized, and then the lyophilizate was hydrated with PBS (pH 7.4) at 50°C. The liposome solution was freeze-thawed for 3 cycles with liquid nitrogen. Then the particle size of the liposomes was adjusted by extrusion through 100-nm pore-size polycarbonate filters (Nuclepore, Cambridge, MA, USA). Unencapsulated FK506 was removed by ultracentrifugation at 604,000 *g* for 15 min (Hitachi, Tokyo, Japan), and the concentration of FK506 in the liposomes was determined by HPLC (Hitachi). Final liposomal concentration was 10 mM as DSPC. FK506-liposomes were dissolved in tetrahydrofuran, and 20 μl of the solution was injected into an octadecylsilane (ODS) column (TSK gel ODS-80TM, 4.6×150 mm, Tosoh, Tokyo, Japan). The mobile phase consisted of acetonitrile and water (3:2, v/v). HPLC analysis was performed at 60°C and a flow rate of 1 ml/min with UV detection at 214 nm. For the cerebral distribution study, 1,1′-dioctadecyl-3,3,3′,3′-tetramethylindocarbocyanine (DiI-C_{18}; Molecular Probes Inc., Eugene, OR, USA) was mixed with the initial lipid solution for fluorescence labeling of the liposomes.

Cell culture

Pheochromocytoma cells [PC12 cells; European Collection of Cell Cultures (ECACC), Porton Down, UK] were cultured in high-glucose DME medium (Wako, Osaka, Japan) supplemented with streptomycin (100 μg/ml), penicillin (100 U/ml), heat-inactivated 5% fetal bovine serum (FBS; Japan Bioserum, Tokyo, Japan), and 10% horse serum (HS; MP Biomedicals, Solon, OH, USA) at 37°C in a humidified chamber with 5% CO_2. PC12 cells were plated on poly-D-lysine-coated 24-well plates for the WST (viability) assay. These cells were caused to differentiate into nerve-like cells by adding nerve growth factor (NGF) at 100 ng/ml to DME medium containing 0.5% HS. Five days after incubation with NGF, these cells were used for subsequent experiments.

Cell proliferation assays

FK506-liposomes (0.01, 0.1, or 1.0 μM as FK506 dosage) or free FK506 (1.0 μM) were added to differentiated PC12 cells in 24-well plates. H_2O_2 was added to each well to a final concentration of 75 μM at 30 min after addition of the samples. The number of viable cells was measured by using TetraColor One (Seikagaku, Tokyo, Japan). Briefly, TetraColar One solution was added to each well, and the cells were then incubated at 37°C for 3 h in a humidified atmosphere containing 5% CO_2. Absorbance at 450 nm was measured by using a Tecan Infinite M200 microplate reader (Tecan, Männedorf, Switzerland). FK506 was dissolved in ethanol, and the final concentration of ethanol was 0.1% in medium.

t-MCAO rats

Preparation of t-MCAO rats was performed as described previously (15). Briefly, anesthesia was induced with 3% isoflurane and maintained with 1.5% isoflurane during surgery. During surgery, the body temperature of the rats was maintained at 37°C with a heating pad. After a median incision of the neck skin had been made, the right carotid artery, external carotid artery, and internal carotid artery (ICA) were isolated with careful conservation of the vagal nerve. An ~18 mm 4-0 monofilament nylon suture coated with silicon was introduced into the right ICA and advanced to the origin of the MCA to occlude it. Silk thread was used for ligation to keep the filament at the site of insertion into the MCA. After the surgery, the neck was closed; anesthesia was then discontinued. MCAO was performed for 1 h. Success of the surgery was judged by the appearance of hemiparesis and an increase in body temperature (>37.8°C). Reperfusion was started by withdrawing the filament ~10 mm at 1 h after the start of occlusion under isoflurane anesthesia.

Drug administration

Polyoxyethylene (60) hydrogenated castor oil (HCO-60; 200 mg/ml), including 10% ethanol was used as vehicle for free FK506. FK506 or FK506-liposomes were intravenously injected at a single dose of 30, 100, or 300 μg/kg body weight (0.5 ml/rat) immediately after the start of reperfusion. In the therapeutic time window study, the injection time was shifted as indicated in the legend of **Fig. 6**. It was reported earlier that the vehicle has no effect on the outcome of ischemia (6, 16, 17).

Cerebral distribution of FK506-liposomes

PEGylated liposomes and FK506-liposomes were fluorescently labeled with DiI-C_{18} as described above. They were intravenously injected into the t-MCAO rats at the start of reperfusion. The rats were euthanized at 3 or 24 h after the injection, and their brains were sliced into 2-mm-thick coronal sections with a rat brain slicer (Muromachi Kikai, Tokyo, Japan). All sections were put on glass slides, and the fluorescence of DiI was measured with an *in vivo* imaging system (IVIS; Xenogen Corp., Alameda, CA, USA). Thereafter, these sections were embedded in optical cutting temperature (OCT) compound (Sakura, Finetech., CO Ltd., Tokyo, Japan) and then frozen in a dry ice/ethanol bath. These frozen sections were cut into 10-μm ones with a cryostat (HM505E; Microm, Walldorf, Germany) for subsequent immunostaining experiments. Average photon counts in I/R region were calculated from 4 rats at each time.

Immunostaining for CD31

The sections were incubated with 1% bovine serum albumin in PBS for 10 min at room temperature for blocking, and then with biotinylated anti-mouse CD31 rat monoclonal antibody (BD Pharmingen, Franklin Lakes, NJ, USA) for 18 h at 4°C, and thereafter with streptavidin-Alexa fluor 488 conjugates (Molecular Probes Inc.) for 30 min at room temperature. Finally, the sections were mounted with Perma Fluor Aqueous Mounting Medium (Thermo Shandon, Pittsburgh, PA, USA) and observed for fluorescence in the striatum with an LSM microscope system (Carl Zeiss Co., Ltd., Oberkochen, Germany).

Terminal deoxyribonucleotidyl transferase (TDT)-mediated dUTP-digoxigenin nick end labeling (TUNEL) staining

Brains of t-MCAO rats were dissected at 24 h after the injection of FK506-liposomes (100 μg/kg as FK506 dosage), free FK506 (100 μg/kg), PEGylated liposomes (same lipid concentration as FK506-liposomes), or PBS; embedded in optimal cutting temperature (OCT) compound (Sakura Finetek, Torrance, CA, USA); and then frozen in dry ice/ethanol. Frozen sections (10 μm) were prepared by using a cryostatic microtome (HM 505E, Microm, Walldorf, Germany) and were stained with TUNEL reagents supplied in an ApopTag Plus fluorescein *in situ* apoptosis detection kit (Chemicon International, Inc., Temecula, CA, USA), as described below. For fixation of the sections, they were incubated in 4% paraformaldehyde for 15 min at room temperature, and then in ethanol/acetic acid (2:1) solution for 5 min at −20°C. DNA strand breaks were labeled with the digoxigenin-conjugated terminal deoxynucleotidyl transferase enzyme by incubation for 1 h at 37°C. Then, the sections were incubated in antidigoxigenin-fluorescein solution for 30 min at room temperature. Finally, the sections were mounted with Perma Fluor aqueous mounting medium including DAPI (1.0 μg/ml) and observed for fluorescence with the LSM system. The observed area in the striatum was similar to the imaged region in **Fig. 2C, D**. For quantitative evaluation, the number of TUNEL-positive cells was counted in 4 sections/rat. Five rats were used to obtain the quantitative data.

Histological analysis of neutrophil influx

Frozen sections (7 μm) were prepared as described above. For fixation of these sections, they were incubated in acetone for 1 min at room temperature, and then in 0.3% H_2O_2 solution for 30 min at room temperature. After having been blocked with fetal bovine serum for 20 min at room temperature, the sections were incubated with anti-myeloperoxidase (MPO) rabbit polyclonal antibody (Thermo Fisher Scientific, Rockford, IL, USA) for 30 min at room temperature. A Vectastain ABC rabbit IgG kit and DAB peroxidase substrate kit (both from Vector Laboratories, Inc., Burlingame, CA, USA) were used for identification of neutrophils in the sections. Finally, the sections were counterstained with hematoxylin and observed microscopically (BX51; Olympus, Tokyo, Japan). The observed area in the striatum was similar to the imaged region in Fig. 2*C, D*.

Therapeutic experiment

FK506-liposomes (30 or 100 μg/kg as FK506 dosage), PBS, free FK506 (30, 100, or 300 μg/kg), or vehicle (200 mg/ml HCO-60 including 10% ethanol in PBS) for FK506 were intravenously injected into t-MCAO rats immediately after the start of reperfusion. The volume of damaged region, the degree of brain swelling, and the functional outcome of rats were assessed at 24 h after the injection. For the functional outcome study, the rats underwent a 21-point neurological score analysis prior to sacrifice, as described previously (18). All of the normal and sham-operated rats received 21 points in this test. After this study, the brains of t-MCAO rats were sliced into 2-mm-thick coronal sections by using a rat brain slicer (Muromachi Kikai) and stained with 2,3,5-triphenyltetrazolium chloride (TTC; Wako) for the detection of cerebral cell death. The volume of the damaged regions was calculated by using an image-analysis system (Image J; U.S. National Institutes of Health, Bethesda, MD, USA). The damaged regions were considered to be those appearing completely white. Brain swelling was calculated as the ratio of volumes between ipsilateral and contralateral hemisphere sections.

Assessment of therapeutic time window

t-MCAO rats were intravenously injected with FK506-liposomes (30 or 100 μg/kg as FK506 dosage) or PBS at various times after the start of reperfusion. The volume of damaged regions was assessed at 24 h after injection by using TTC staining as described above.

Statistical analysis

Statistical analysis was performed by 1-way analysis of variance (ANOVA) followed by Dunnett's multiple comparison tests. Data are presented as means ± SD.

RESULTS

FK506-liposomes protected differentiated PC12 cells from H_2O_2-induced toxicity

The particle size and ζ-potential of FK506 liposomes were 109 ± 4.3 nm and −7.2 ± 0.7 mV, respectively. To

assess the pharmacological activity of FK506-liposomes, we examined the cytoprotective effect of them on differentiated PC12 cells treated with H_2O_2. The number of live PC12 cells was decreased to ~40% by exposure to H_2O_2 (**Fig. 1**). FK506-liposomes suppressed this cell death induced by H_2O_2 in a dose-dependent manner, whereas empty-liposomes (PEGylated liposomes) showed no cytoprotective effect against the H_2O_2-induced toxicity.

FK506-liposomes diffused into the brain parenchyma only in the ischemic hemisphere

The intracerebral distribution of FK506-liposomes given immediately after the start of reperfusion to t-MCAO rats was observed at 3 h (Fig. 2*A*) and 24 h (Fig. 2*B*) after the injection. The fluorescence of DiI-labeled FK506-liposomes was observed only in the ischemic hemisphere at both time points. Immunohistological analysis revealed that the FK506-liposomes had leaked into the brain parenchyma from cerebral vessels in the ipsilateral hemisphere (Fig. 2*C, D*). Moreover, higher DiI fluorescence intensity was detected in the brain sections prepared at 24 h after the injection than in those prepared at 3 h (Fig. 2*E*) after it, which suggests that the accumulation of FK506-liposomes in the brain parenchyma gradually increased by continuous leakage from cerebral vessels according to enhanced permeability and the retention effect. In contrast, no leakage of them into the cerebral parenchyma of the contralateral hemisphere occurred.

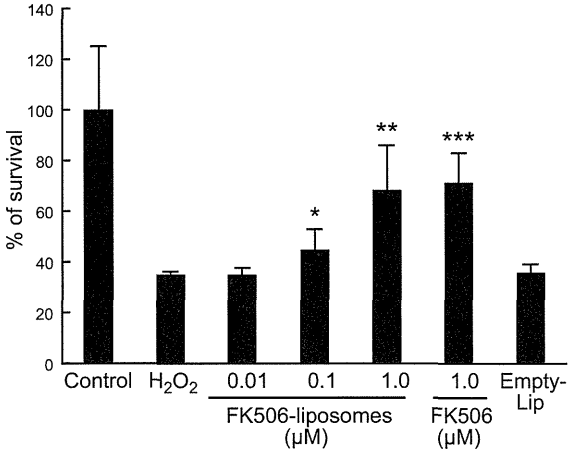

Figure 1. FK506-liposome-mediated attenuation of H_2O_2-induced cytotoxicity toward differentiated PC12 cells. PC12 cells were caused to differentiate by the addition of NGF at 100 ng/ml to culture medium supplemented with 0.5% HS. After 5 d in culture for differentiation, FK506-liposomes, free FK506, or empty liposomes (Empty-Lip) were added to the culture medium, and then H_2O_2 was added to each well. After 24 h, viable cell numbers were determined by performing the WST assay. Final lipid concentration of empty liposomes was same as that of FK506-liposomes. Data are presented as means ± SD (n=6). $^*P < 0.05$, $^{**}P < 0.01$, $^{***}P < 0.001$ *vs.* H_2O_2-treated group.

FK506-liposomes showed antiapoptotic effect in t-MCAO rats

At 24 h after the injection of each sample, apoptosis of the cerebral cells in t-MCAO rats was identified by TUNEL staining (**Fig. 3**). TUNEL-positive cells were detected in neither the striatum nor the cerebral cortex in the nonischemic hemisphere (data not shown). A number of apoptotic cells were observed in the control group and free FK506-treated group (Fig. 3*A, B*). This dosage (100 μg/kg) of free FK506 was too low to exert an antiapoptotic effect in t-MCAO rats. However, FK506-liposomes obviously reduced the number of TUNEL-positive cells despite the same dosage as free FK506. Quantitative analysis of TUNEL-positive cells elucidated the difference between each group (Fig. 3*C*). In the FK506-liposome-treated group, the number of apoptotic cells in the striatum was significantly reduced compared with that in the other groups. In contrast to this result, there was no significant difference in the cortex between FK506-liposome-treated group and other groups, even though this treatment tended to suppress the cerebral apoptosis. Empty liposomes had no effect on apoptosis induced by I/R injury.

FK506-liposomes suppressed neutrophil invasion induced by I/R

To evaluate anti-inflammatory effect of FK506-liposomes, we examined neutrophil invasion into I/R regions as an indicator of intracerebral inflammation (**Fig. 4**). In the nonischemic hemisphere of all groups, almost no MPO-stained cells were identified (data not shown). Conversely, a number of neutrophils that had infiltrated were detected in the striatum and the cortex of the ischemic hemisphere (Fig. 4*A*, control). In the FK506-liposome-treated group, few MPO-positive cells were observed in the striatum, whereas they were more numerous in the cortex. The quantitative analysis revealed that FK506-liposomes reduced the number of infiltrating neutrophils in the striatum by ~80%, and significantly suppressed neutrophil invasion compared with the treatment with the same dosage of free FK506 (Fig. 4*B*).

FK506-liposomes ameliorated cerebral I/R injury in t-MCAO rats

t-MCAO caused cerebral cell death and brain swelling in these experimental model rats. Treatment with free FK506 at 30 or 100 μg/kg hardly affected the damaged region and brain swelling induced by I/R, whereas FK506-liposomes at these same dosages as the free drug significantly reduced the amount of brain damage (**Fig. 5A, B**). Furthermore, administration of FK506-liposomes at 100 μg/kg showed therapeutic efficacy quite similar to that obtained with the free drug at 300 μg/kg. These results suggest that liposomalization of FK506 enhanced its cytoprotective

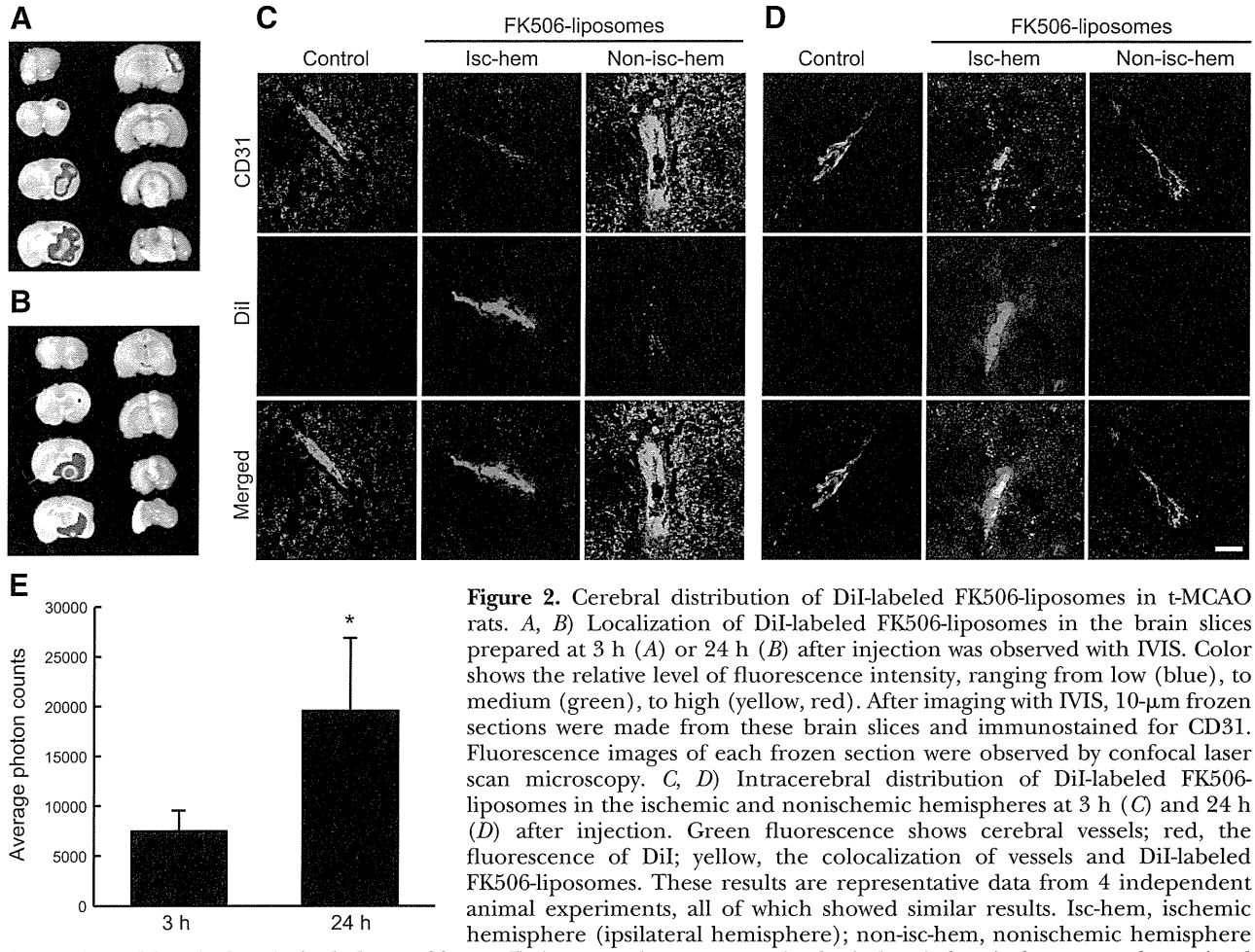

Figure 2. Cerebral distribution of DiI-labeled FK506-liposomes in t-MCAO rats. *A, B*) Localization of DiI-labeled FK506-liposomes in the brain slices prepared at 3 h (*A*) or 24 h (*B*) after injection was observed with IVIS. Color shows the relative level of fluorescence intensity, ranging from low (blue), to medium (green), to high (yellow, red). After imaging with IVIS, 10-μm frozen sections were made from these brain slices and immunostained for CD31. Fluorescence images of each frozen section were observed by confocal laser scan microscopy. *C, D*) Intracerebral distribution of DiI-labeled FK506-liposomes in the ischemic and nonischemic hemispheres at 3 h (*C*) and 24 h (*D*) after injection. Green fluorescence shows cerebral vessels; red, the fluorescence of DiI; yellow, the colocalization of vessels and DiI-labeled FK506-liposomes. These results are representative data from 4 independent animal experiments, all of which showed similar results. Isc-hem, ischemic hemisphere (ipsilateral hemisphere); non-isc-hem, nonischemic hemisphere (contralateral hemisphere). Scale bar = 20 μm. *E*) Average photon counts in the ischemic hemisphere were determined by the image of brain slices with IVIS (n=4). *$P < 0.05$.

effect due to improved biodistribution. In accordance with several reports, the extent of cerebral cell death, as indicated by reduced brain volume (Fig. 5*A*), and that of brain swelling (Fig. 5*B*) were similar in both control (PBS-injected) and vehicle-injected groups.

The therapeutic time window (TTW) of agents is critical information for developing neuroprotectants, particularly in designing the clinical trial. The TTW of FK506-liposomes was estimated by altering the time of injection after the commencement of reperfusion (Fig. 6). The volume of brain damage in the t-MCAO rats was significantly decreased by the dose of FK506-liposomes administered at 30 μg/kg as FK506 up through 2 h after reperfusion had begun. However, the treatment with the same dose of FK506-liposomes given at 3 h after the start of reperfusion or later had almost no effect on cerebral cell death, as judged by the results of TTC staining. Moreover, a higher amount of FK506-liposomes (100 μg/kg as FK506) injected at 3 h after reperfusion had begun also scarcely suppressed the brain damage. Taken together, these data indicate that the therapeutic time window for FK506-liposomes was up to 2 h after MCAO/reperfusion in this experimental model rat, and suggest that the injection of them at an early time would result in a good outcome.

The motor ability of the t-MCAO rats was evaluated based on the 21-point motor score (**Fig. 7**). In the control group, hemiparesis was observed at 24 h after the start of reperfusion, resulting in a low score. On the other hand, t-MCAO rats treated with FK506-liposomes showed alleviated hemiparesis, especially in their hind legs. This recovery probably contributed to the high scores on the inclined platform test, horizontal bar test (forepaws placed on ribbed bar), and circling test obtained for the FK506-liposome-treated animals (Supplemental Table S1). The administration of free FK506 at 300 μg/kg also significantly improved motor function deficit. These results correlated well with the extent of cerebral cell death and swelling.

DISCUSSION

The present study showed that FK506-liposomes significantly suppressed neutrophil invasion and apoptotic cell death, and ameliorated neurological deficits in t-MCAO rats compared with free FK506. The liposomalization of FK506 might lead to an increase in the amount of drug accumulation in I/R regions. The disruption of blood-brain barrier is induced at an early

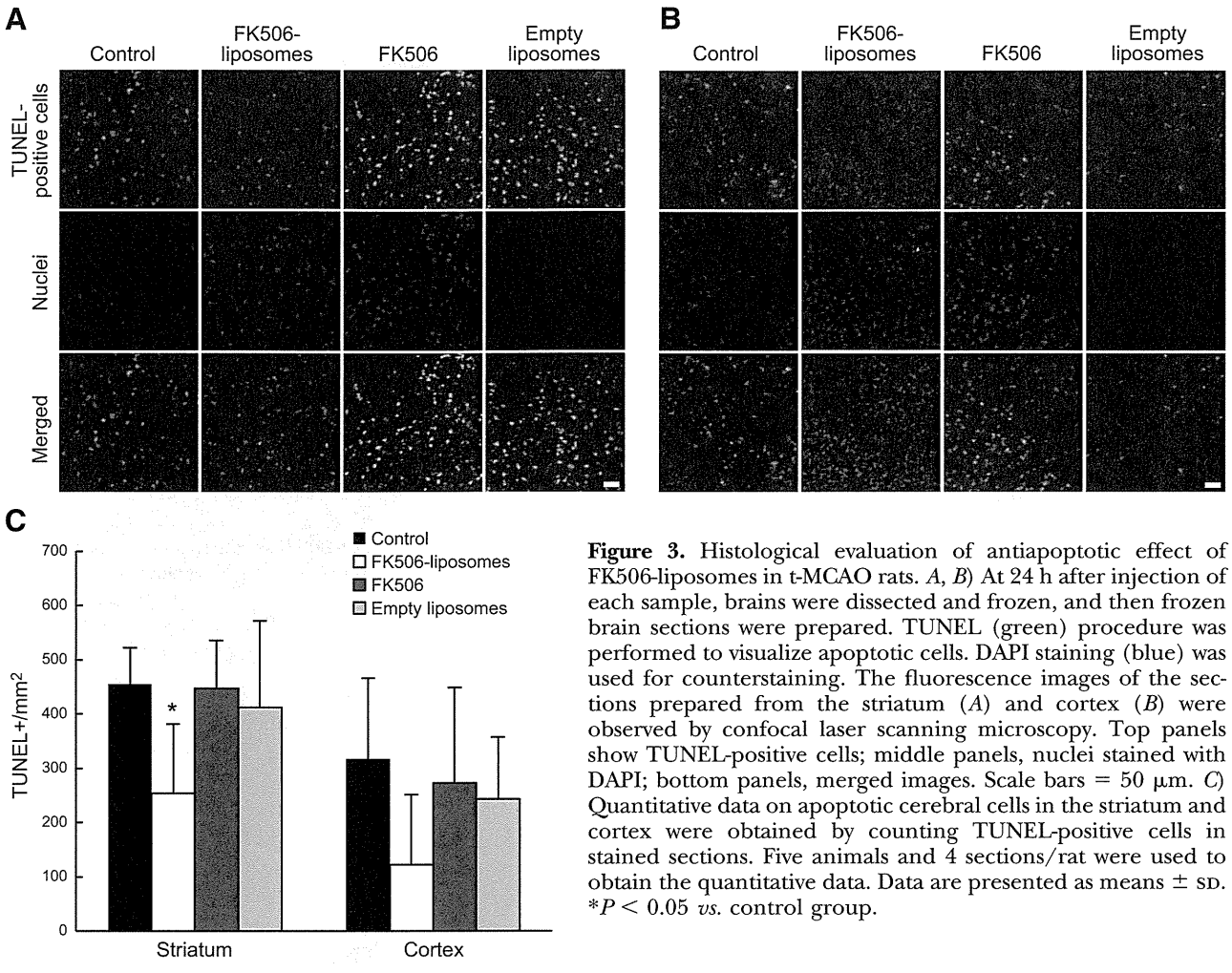

Figure 3. Histological evaluation of antiapoptotic effect of FK506-liposomes in t-MCAO rats. *A, B*) At 24 h after injection of each sample, brains were dissected and frozen, and then frozen brain sections were prepared. TUNEL (green) procedure was performed to visualize apoptotic cells. DAPI staining (blue) was used for counterstaining. The fluorescence images of the sections prepared from the striatum (*A*) and cortex (*B*) were observed by confocal laser scanning microscopy. Top panels show TUNEL-positive cells; middle panels, nuclei stained with DAPI; bottom panels, merged images. Scale bars = 50 μm. *C*) Quantitative data on apoptotic cerebral cells in the striatum and cortex were obtained by counting TUNEL-positive cells in stained sections. Five animals and 4 sections/rat were used to obtain the quantitative data. Data are presented as means ± SD. $^{*}P < 0.05$ *vs.* control group.

stage in the ischemic core region after cerebral ischemia (19, 20). Moreover, a previous report demonstrated that the area in which macromolecules accumulate expands as time passes after I/R in t-MCAO rats (21). Hence, the concept of passive targeting, as constructed for cancer treatment, could be a promising scheme for efficient drug delivery to I/R regions. In the present study, a higher extent of localization of FK506-liposomes in the ischemic hemisphere was observed at 24 h than at 3 h after the injection. This result suggests that the accumulation amount of FK506-liposomes given at the start of reperfusion gradually increased in

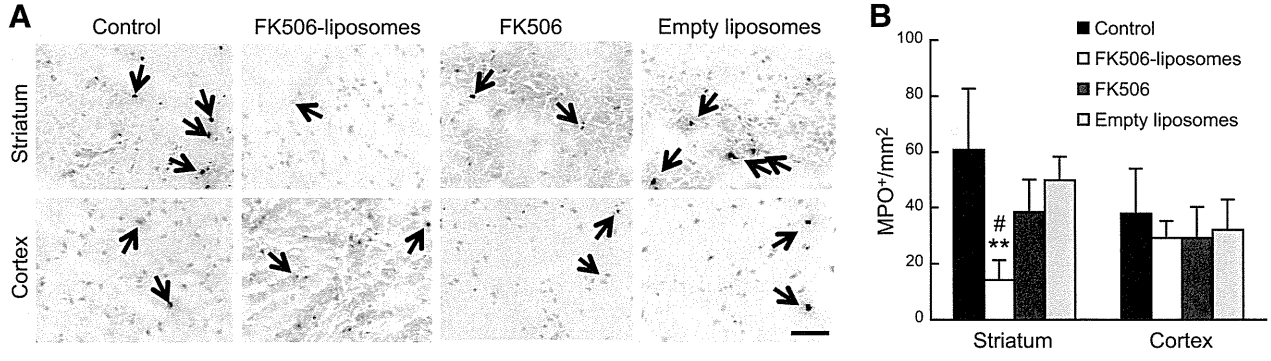

Figure 4. Invasion of neutrophils into the brain parenchyma of t-MCAO rats. At 24 h after injection of each sample, brains were dissected and frozen; and then frozen brain sections were prepared. MPO immunostaining was performed to visualize neutrophils (brown). Hematoxylin staining (blue) was used for counterstaining. *A*) Stained sections were observed by microscopy. Arrows indicate neutrophils that had infiltrated the brain parenchyma. Scale bar = 50 μm. *B*) Quantitative data on neutrophil invasion analysis were obtained by counting MPO-positive cells in stained sections. Data are presented as means ± SD (n=6). $^{**}P < 0.01$ *vs.* control group; $^{\#}P < 0.05$ *vs.* free FK506-treated group.

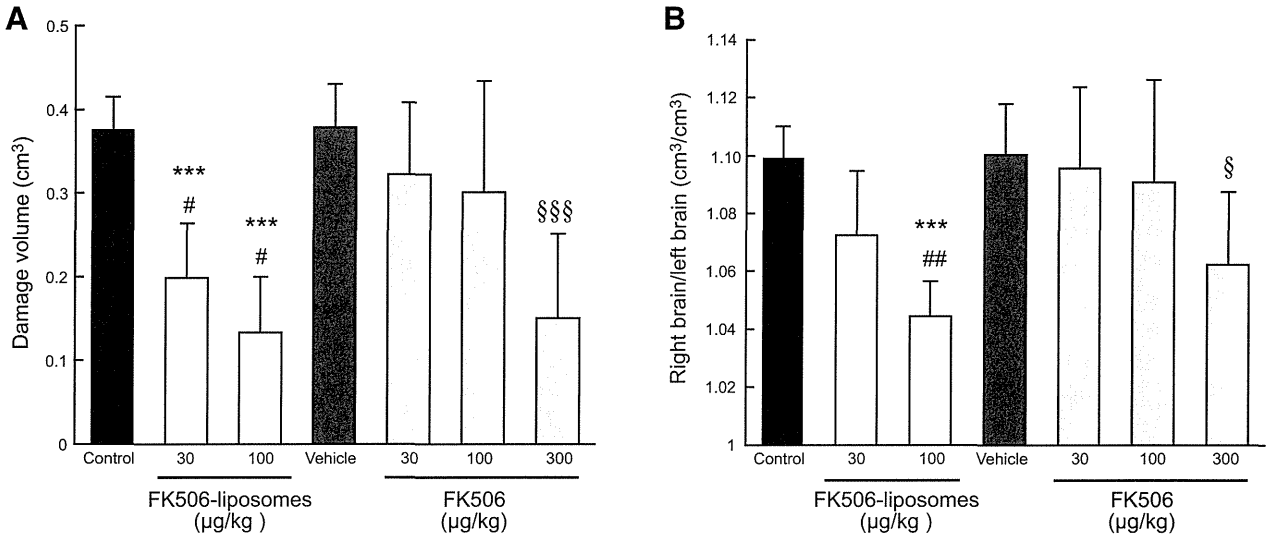

Figure 5. Suppression of cerebral cell death and brain swelling by the treatment with FK506-liposomes. t-MCAO rats were injected *via* a tail vein with PBS, FK506-liposomes, vehicle for free FK506 or free FK506 immediately after the start of reperfusion at dosages indicated as FK506. At 24 h after injection, brains were dissected and stained with TTC. Damage volume (*A*) and degree of brain swelling (*B*) were calculated by using Image J. Data are means ± SD (n=7). $^{***}P < 0.001$ *vs.* control group; $^{\#}P < 0.05$, $^{\#\#}P < 0.01$ *vs.* free FK506-treated group at the same dose; $^{\S}P < 0.05$, $^{\S\S\S}P < 0.001$ *vs.* vehicle-treated group.

a time-dependent manner, as in the case of enhanced permeability and retention effect. However, the half-life of free FK506 is extremely short, and FK506 administered intravenously is almost totally metabolized by the liver, primarily by cytochrome P450 3A (22, 23). The change in biodistribution afforded by liposomalization would be expected to be closely related to the therapeutic outcome.

Fatal damage in the striatum, the region assumed to be the ischemic core in the present experimental model, occurs at an early stage after an I/R event (21). In this study, FK506-liposomes substantially reduced the cerebral cell death and inflammation induced by I/R in this region. Thus, FK506-liposomes spreading into the brain parenchyma quickly showed pharmacological activity. Although PEG-modification of liposomes prolongs their circulation in the blood, it causes a decrease in cellular uptake of liposomes (24, 25). Therefore, FK506-liposomes reaching I/R regions might have released FK506 into the brain parenchyma, and the released drugs then acted on the cerebral cells.

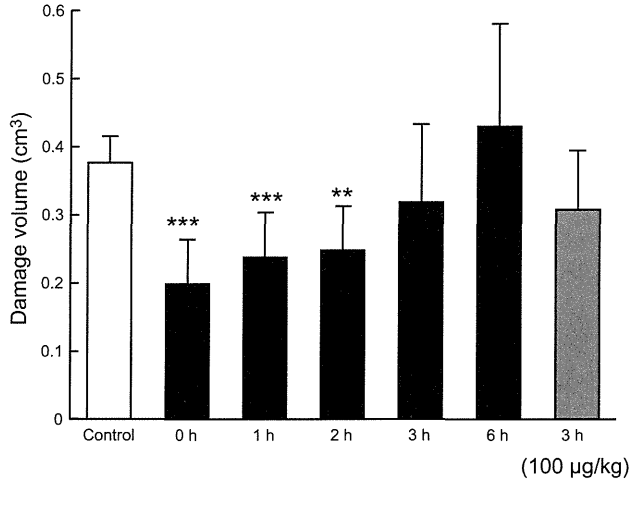

Figure 6. Therapeutic time window of FK506-liposomes in t-MCAO rats. t-MCAO rats were intravenously injected *via* a tail vein with FK506-liposomes (30 or 100 μg/kg as FK506 dosage) at the indicated times (0, 1, 2, 3, or 6 h) after the start of reperfusion. At 24 h after reperfusion had begun, brain was dissected and stained with TTC. Damage volume was calculated by using Image J. Data are presented as means ± SD (n=6–7). $^{**}P < 0.01$, $^{***}P < 0.001$ *vs.* control.

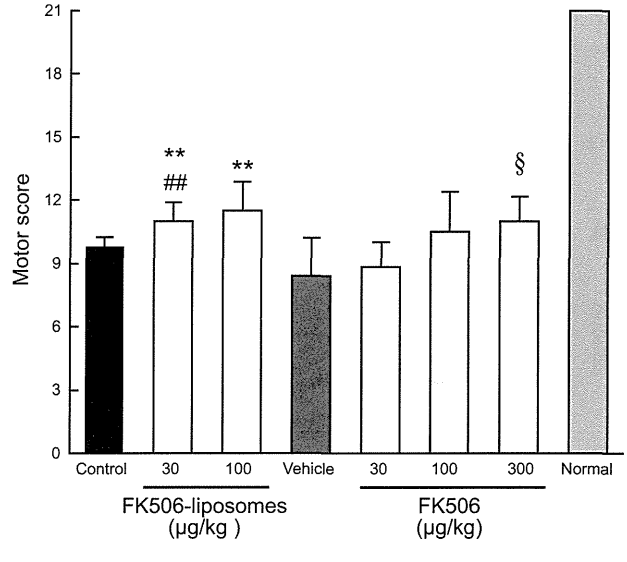

Figure 7. Motor activity score of t-MCAO rats. t-MCAO rats were treated with each sample as described in the legend of Fig. 5, and these rats were then assessed for motor function in a 21-point neuropathological scoring system. Data are presented as means ± SD (n=7). $^{**}P < 0.01$ *vs.* control group; $^{\#\#}P < 0.01$ *vs.* free FK506-treated group at the same dose; $^{\S}P < 0.05$ *vs.* vehicle-treated group.

Neutrophils generate cytotoxic substances such as hypochlorous acid in inflammation sites, resulting in progressive inflammation. These cells normally do not exist in the brain, but they do invade into the cerebral parenchyma *via* brain endothelial cells after a cerebral ischemic event. This invasion induced by intracerebral inflammation occurs during the period of 9 to 24 h after the start of reperfusion in t-MCAO rats (26). Therefore, the observation of neutrophil invasion is one way to assess the extent of cerebral inflammation after I/R. In the present study, FK506-liposomes significantly suppressed the neutrophil invasion induced by cerebral I/R. A past study showed that FK506 inhibits the expression of adhesion molecules in the cerebral vasculature by reducing the production of inflammatory cytokines by neuronal cells and glia cells (26). Accordingly, we suggest that FK506-liposomes administered after the start of reperfusion inhibited the inflammatory response by affecting neuronal cells and glia cells in the t-MCAO rats.

FK506 directly suppresses apoptotic cell death induced by cerebral I/R through the inhibition of Bad dephosphorylation and subsequent cytochrome *c* release (27, 28). In addition, the prevention of reactive oxygen species production is related to its antiapoptotic effect on cerebral cells injured by I/R (29). The present study demonstrated that FK506-liposomes markedly reduced the number of apoptotic cells in t-MCAO rats. These multifunctional mechanisms, including the anti-inflammatory effect of FK506-liposomes, probably effectively acted on the neurovascular unit to bring about the good outcome in the t-MCAO rats.

A large number of small molecules as neuroprotectants have failed in clinical trials (30). Based on our present data, we propose that liposomalization of small molecular neuroprotectants should overcome their insufficiency of medicinal efficacy and adverse side effects. Liposomes can encapsulate many kinds of drugs regardless of their being hydrophilic or hydrophobic. Furthermore, liposomes can be modified with functional molecules, resulting in improved biodistribution, controlled release of drugs, increase in drug accumulation in targeted cells, regulation of intracellular distribution, and so on (31–34). Therefore, liposomal DDS has a great potential to be a novel strategy for the treatment of cerebral I/R injury.

In summary, our data demonstrate the usefulness of FK506-liposomes for the treatment of cerebral ischemia/reperfusion injury. FK506-liposomes intravenously injected immediately after the start of reperfusion significantly suppressed neutrophil invasion, apoptotic cell death, and infarct volume compared with free FK506 in t-MCAO rats. In addition, the motor function deficits induced by ischemia/reperfusion in these rats were ameliorated to a greater extent by the treatment with FK506-liposomes than by that with free FK506. Therefore, liposomalization of FK506 should permit a reduction in the dosage of FK506 without a decrease in the therapeutic efficacy of the drug. Taken together, our present findings indicate that FK506-liposomes have a clear potential to be a neuroprotectant if administered quickly after a cerebral stroke. FJ

The authors thank Astellas Pharmaceutical Co., Ltd. (Tokyo, Japan) for the gift of the FK506. This research was supported by a grant-in-aid for scientific research from the Japan Society for the Promotion of Science.

REFERENCES

1. Wong, C. H., and Crack, P. J. (2008) Modulation of neuroinflammation and vascular response by oxidative stress following cerebral ischemia-reperfusion injury. *Curr. Med. Chem.* **15,** 1–14
2. Eltzschig, H. K., and Eckle, T. (2011) Ischemia and reperfusion–from mechanism to translation. *Nat. Med.* **17,** 1391–1401
3. Tuma, R. F., and Steffens, S. (2012) Targeting the endocannabinod system to limit myocardial and cerebral ischemic and reperfusion injury. *Curr. Pharm. Biotechnol.* **13,** 46–58
4. Ginsberg, M. D. (2009) Current status of neuroprotection for cerebral ischemia: synoptic overview. *Stroke* **40,** S111–114
5. Ishii, T., Asai, T., Oyama, D., Fukuta, T., Yasuda, N., Shimizu, K., Minamino, T., and Oku, N. (2012) Amelioration of cerebral ischemia-reperfusion injury based on liposomal drug delivery system with asialo-erythropoietin. *J. Control. Release* **160,** 81–87
6. Sharkey, J., and Butcher, S. P. (1994) Immunophilins mediate the neuroprotective effects of FK506 in focal cerebral ischaemia. *Nature* **371,** 336–339
7. Furuichi, Y., Maeda, M., Moriguchi, A., Sawamoto, T., Kawamura, A., Matsuoka, N., Mutoh, S., and Yanagihara, T. (2003) Tacrolimus, a potential neuroprotective agent, ameliorates ischemic brain damage and neurologic deficits after focal cerebral ischemia in nonhuman primates. *J. Cereb. Blood Flow Metab.* **23,** 1183–1194
8. Szydlowska, K., Zawadzka, M., and Kaminska, B. (2006) Neuroprotectant FK506 inhibits glutamate-induced apoptosis of astrocytes in vitro and in vivo. *J. Neurochem.* **99,** 965–975
9. Morioka, M., Hamada, J., Ushio, Y., and Miyamoto, E. (1999) Potential role of calcineurin for brain ischemia and traumatic injury. *Prog. Neurobiol.* **58,** 1–30
10. Wang, H. G., Pathan, N., Ethell, I. M., Krajewski, S., Yamaguchi, Y., Shibasaki, F., McKeon, F., Bobo, T., Franke, T. F., and Reed, J. C. (1999) Ca2+-induced apoptosis through calcineurin dephosphorylation of BAD. *Science* **284,** 339–343
11. Hashiguchi, A., Kawano, T., Yano, S., Morioka, M., Hamada, J., Sato, T., Shirasaki, Y., Ushio, Y., and Fukunaga, K. (2003) The neuroprotective effect of a novel calmodulin antagonist, 3-[2-[4-(3-chloro-2-methylphenyl)-1-piperazinyl]ethyl]-5,6-dimethoxy-1-(4-imidazolylmethyl)-1H-indazole dihydrochloride 3.5 hydrate, in transient forebrain ischemia. *Neuroscience* **121,** 379–386
12. Kaminska, B., Gaweda-Walerych, K., and Zawadzka, M. (2004) Molecular mechanisms of neuroprotective action of immunosuppressants–facts and hypotheses. *J. Cell. Mol. Med.* **8,** 45–58
13. Chuang, Y. C., Tyagi, P., Huang, H. Y., Yoshimura, N., Wu, M., Kaufman, J., and Chancellor, M. B. (2011) Intravesical immune suppression by liposomal tacrolimus in cyclophosphamide-induced inflammatory cystitis. *Neurourol. Urodyn.* **30,** 421–427
14. Moffatt, S. D., McAlister, V., Calne, R. Y., and Metcalfe, S. M. (1999) Potential for improved therapeutic index of FK506 in liposomal formulation demonstrated in a mouse cardiac allograft model. *Transplantation* **67,** 1205–1208
15. Longa, E. Z., Weinstein, P. R., Carlson, S., and Cummins, R. (1989) Reversible middle cerebral artery occlusion without craniectomy in rats. *Stroke* **20,** 84–91
16. Zhang, N., Komine-Kobayashi, M., Tanaka, R., Liu, M., Mizuno, Y., and Urabe, T. (2005) Edaravone reduces early accumulation of oxidative products and sequential inflammatory responses after transient focal ischemia in mice brain. *Stroke* **36,** 2220–2225
17. Toung, T. J., Bhardwaj, A., Dawson, V. L., Dawson, T. M., Traystman, R. J., and Hurn, P. D. (1999) Neuroprotective FK506 does not alter in vivo nitric oxide production during ischemia and early reperfusion in rats. *Stroke* **30,** 1279–1285

18. Hunter, A. J., Hatcher, J., Virley, D., Nelson, P., Irving, E., Hadingham, S. J., and Parsons, A. A. (2000) Functional assessments in mice and rats after focal stroke. *Neuropharmacology* **39,** 806–816
19. Rosenberg, G. A., Estrada, E. Y., and Dencoff, J. E. (1998) Matrix metalloproteinases and TIMPs are associated with blood-brain barrier opening after reperfusion in rat brain. *Stroke* **29,** 2189–2195
20. Dirnagl, U., Iadecola, C., and Moskowitz, M. A. (1999) Pathobiology of ischaemic stroke: an integrated view. *Trends Neurosci.* **22,** 391–397
21. Ishii, T., Asai, T., Urakami, T., and Oku, N. (2010) Accumulation of macromolecules in brain parenchyma in acute phase of cerebral infarction/reperfusion. *Brain Res.* **1321,** 164–168
22. Yura, H., Yoshimura, N., Hamashima, T., Akamatsu, K., Nishikawa, M., Takakura, Y., and Hashida, M. (1999) Synthesis and pharmacokinetics of a novel macromolecular prodrug of Tacrolimus (FK506), FK506-dextran conjugate. *J. Control. Release* **57,** 87–99
23. Shiraga, T., Matsuda, H., Nagase, K., Iwasaki, K., Noda, K., Yamazaki, H., Shimada, T., and Funae, Y. (1994) Metabolism of FK506, a potent immunosuppressive agent, by cytochrome P450 3A enzymes in rat, dog and human liver microsomes. *Biochem. Pharmacol.* **47,** 727–735
24. Duzgune, scedil, and Nir, S. (1999) Mechanisms and kinetics of liposome-cell interactions. *Adv. Drug Deliv. Rev.* **40,** 3–18
25. Vertut-Doi, A., Ishiwata, H., and Miyajima, K. (1996) Binding and uptake of liposomes containing a poly(ethylene glycol) derivative of cholesterol (stealth liposomes) by the macrophage cell line J774: influence of PEG content and its molecular weight. *Biochim. Biophys. Acta* **1278,** 19–28
26. Noto, T., Furuichi, Y., Ishiye, M., Matsuoka, N., Aramori, I., Mutoh, S., and Yanagihara, T. (2007) Tacrolimus (FK506) limits accumulation of granulocytes and platelets and protects against brain damage after transient focal cerebral ischemia in rat. *Biol. Pharm. Bull.* **30,** 313–317
27. Li, J. Y., Furuichi, Y., Matsuoka, N., Mutoh, S., and Yanagihara, T. (2006) Tacrolimus (FK506) attenuates biphasic cytochrome c release and Bad phosphorylation following transient cerebral ischemia in mice. *Neuroscience* **142,** 789–797
28. Shichinohe, H., Kuroda, S., Abumiya, T., Ikeda, J., Kobayashi, T., Yoshimoto, T., and Iwasaki, Y. (2004) FK506 reduces infarct volume due to permanent focal cerebral ischemia by maintaining BAD turnover and inhibiting cytochrome c release. *Brain Res.* **1001,** 51–59
29. Dawson, T. M., Steiner, J. P., Dawson, V. L., Dinerman, J. L., Uhl, G. R., and Snyder, S. H. (1993) Immunosuppressant FK506 enhances phosphorylation of nitric oxide synthase and protects against glutamate neurotoxicity. *Proc. Natl. Acad. Sci. U. ¦S. ¦A.* **90,** 9808–9812
30. Sahota, P., and Savitz, S. I. (2011) Investigational therapies for ischemic stroke: neuroprotection and neurorecovery. *Neurotherapeutics* **8,** 434–451
31. Asai, T., Matsushita, S., Kenjo, E., Tsuzuku, T., Yonenaga, N., Koide, H., Hatanaka, K., Dewa, T., Nango, M., Maeda, N., Kikuchi, H., and Oku, N. (2011) Dicetyl phosphate-tetraethylenepentamine-based liposomes for systemic siRNA delivery. *Bioconjug. Chem.* **22,** 429–435
32. Tan, M. L., Choong, P. F., and Dass, C. R. (2010) Recent developments in liposomes, microparticles and nanoparticles for protein and peptide drug delivery. *Peptides* **31,** 184–193
33. Torres, E., Mainini, F., Napolitano, R., Fedeli, F., Cavalli, R., Aime, S., and Terreno, E. (2011) Improved paramagnetic liposomes for MRI visualization of pH triggered release. *J. Control. Release* **154,** 196–202
34. Micheli, M. R., Bova, R., Magini, A., Polidoro, M., and Emiliani, C. (2012) Lipid-based nanocarriers for CNS-targeted drug delivery. *Recent Pat. CNS Drug Discov.* **7,** 71–86

Received for publication October 1, 2012.
Accepted for publication December 4, 2012.

Am J Physiol Heart Circ Physiol 304: H1361–H1369, 2013.
First published March 15, 2013; doi:10.1152/ajpheart.00454.2012.

Dipeptidyl-peptidase IV inhibition improves pathophysiology of heart failure and increases survival rate in pressure-overloaded mice

Ayako Takahashi,[1,4] Masanori Asakura,[2] Shin Ito,[1] Kyung-Duk Min,[1] Kazuhiro Shindo,[1,4] Yi Yan,[4] Yulin Liao,[6] Satoru Yamazaki,[1] Shoji Sanada,[5] Yoshihiro Asano,[4,5] Hatsue Ishibashi-Ueda,[3] Seiji Takashima,[4,5] Tetsuo Minamino,[5] Hiroshi Asanuma,[7] Naoki Mochizuki,[1] and Masafumi Kitakaze[2]

[1]Department of Cell Biology, [2]Department of Clinical Research and Development, and [3]Division of Pathology, National Cerebral and Cardiovascular Center, Osaka, Japan; [4]Department of Molecular Cardiology and [5]Department of Cardiovascular Medicine, Osaka University Graduate School of Medicine, Osaka, Japan; [6]Department of Cardiology, Nanfang Hospital, Southern Medical University, Guangzhou, China; and [7]Department of Cardiology, Kyoto Prefectural University School of Medicine, Kyoto, Japan

Submitted 12 June 2012; accepted in final form 25 January 2013

Takahashi A, Asakura M, Ito S, Min KD, Shindo K, Yan Y, Liao Y, Yamazaki S, Sanada S, Asano Y, Ishibashi-Ueda H, Takashima S, Minamino T, Asanuma H, Mochizuki N, Kitakaze M. Dipeptidyl-peptidase IV inhibition improves pathophysiology of heart failure and increases survival rate in pressure-overloaded mice. *Am J Physiol Heart Circ Physiol* 304: H1361–H1369, 2013. First published March 15, 2013; doi:10.1152/ajpheart.00454.2012.—Incretin hormones, including glucagon-like peptide-1 (GLP-1), a target for diabetes mellitus (DM) treatment, are associated with cardioprotection. As dipeptidyl-peptidase IV (DPP-IV) inhibition increases plasma GLP-1 levels in vivo, we investigated the cardioprotective effects of the DPP-IV inhibitor vildagliptin in a murine heart failure (HF) model. We induced transverse aortic constriction (TAC) in C57BL/6J mice, simulating pressure-overloaded cardiac hypertrophy and HF. TAC or sham-operated mice were treated with or without vildagliptin. An intraperitoneal glucose tolerance test revealed that blood glucose levels were higher in the TAC than in sham-operated mice, and these levels improved with vildagliptin administration in both groups. Vildagliptin increased plasma GLP-1 levels in the TAC mice and ameliorated TAC-induced left ventricular enlargement and dysfunction. Vildagliptin palliated both myocardial apoptosis and fibrosis in TAC mice, demonstrated by histological, gene and protein expression analyses, and improved survival rate on *day 28* (TAC with vildagliptin, 67.5%; TAC without vildagliptin, 41.5%; $P < 0.05$). Vildagliptin improved cardiac dysfunction and overall survival in the TAC mice, both by improving impaired glucose tolerance and by increasing GLP-1 levels. DPP-IV inhibitors represent a candidate treatment for HF patients with or without DM.

heart failure; impaired glucose tolerance; dipeptidyl-peptidase IV inhibitor

HEART FAILURE (HF) is a leading causes of death in humans worldwide (1, 20, 37, 56), and is often linked to impaired glucose tolerance or diabetes mellitus (DM) (21, 53). DM is a major risk factor for cardiac dysfunction; Lind et al. (28) reported that poor glycemic control among patients with type 1 DM led to a high incidence of cardiovascular events. The energetic substrate utilization of cardiomyocytes under hyperglycemic conditions shifts from glucose to fatty acid oxidation, leading to HF (38). In DM, oxidative stress also causes endothelial dysfunction and decreases endothelial NO release, inducing microangiopathy (13, 31). Either glucose abnormalities or diabetes commonly exists in patients with HF, but as previously reported, patients with diabetes have no worse outcome of HF (50). Our previous clinical study revealed that ~90% of patients with chronic HF had impaired glucose tolerance (21).

Incretin hormones have recently been proposed as new targets for DM treatment. Glucagon-like peptide-1 (GLP-1) is an incretin hormone secreted from the lower intestines and colon, which stimulates insulin secretion from pancreatic beta cells. Its receptors are ubiquitously expressed, including in the cardiovascular system (8). GLP-1 is thought to possess cardioprotective properties because of the following three reasons: *1*) GLP-1 receptors localize to cardiomyocytes and endothelial cells (3, 57); *2*) activation of GLP-1 receptors increases phosphoinositide 3 (PI3)-kinase, serine/threonine protein kinase Akt (Akt), and extracellular signal-regulated kinase phosphorylation, potentially mediating cardioprotection (6, 19); and *3*) activation of GLP-1 receptors stimulates p38 mitogen-activated protein (MAP) kinase and endothelial nitric oxide synthase via protein kinase A activation, putatively affecting cardioprotection (5, 59) and plasma glucose normalization (16). As dipeptidyl-peptidase IV (DPP-IV) rapidly degrades GLP-1, which has a biological half-life of approximately 1.5–5 min (11, 18), both GLP-1 analogs and DPP-IV inhibitors have been developed as new drugs to treat type 2 DM. GLP-1 analogs reportedly ameliorate not only DM but also HF and myocardial ischemia (15, 33, 34, 48, 59), suggesting that DPP-IV inhibitors function cardioprotectively. Indeed, DPP-IV inhibitors are reportedly effective against myocardial infarction in mice and pacing-induced heart failure in pigs (14, 42, 59), suggesting that DPP-IV inhibitors may also affect the survival rate. However, the effects of DPP-IV inhibitors on the pathophysiology of pressure-overloaded HF and survival after HF are unknown.

We aimed to clarify whether vildagliptin, a DPP-IV inhibitor, improves the pathophysiology of HF and increases survival rate in pressure-overloaded mice.

METHODS

All of the animal care procedures were performed according to the American Physiological Society "Guiding Principles in the Care and Use of Vertebrate Animals in Research and Training" and with the approval of the ethical committee of Osaka University.

Address for reprint requests and other correspondence: M. Asakura, Dept. of Clinical Research and Development, National Cerebral and Cardiovascular Center, 5-7-1, Fujishirodai, Suita, Osaka, 565-8565 Japan (e-mail: masakura@ncvc.go.jp).

Animal preparation. Male C57BL/6J mice (8 wk old, weighing 22–24 g) were purchased from CLEA Japan, (Tokyo, Japan). After 1 wk of observation, either transverse aortic constriction (TAC) or a sham operation was performed as previously described (24). In brief, the transverse aorta was isolated between the carotid arteries and constricted by a 7-0 silk suture ligature tied firmly against a 30-gauge needle. Sham-operated mice underwent a similar surgical procedure without aortic constriction. The needle was promptly removed, and the chest was closed with a 5-0 silk suture. Each surgical procedure was completed within 30 min to maintain the body temperature at 37°C.

Experimental protocol. Vildagliptin was gifted by Novartis Pharmaceuticals (Basel, Switzerland). The sham-operated or TAC mice were randomly divided into two subgroups; the sham-operated group with (n = 10) or without vildagliptin (n = 10) and TAC with (n = 40) or without vildagliptin (n = 41). The vildagliptin treatment subgroups were provided with drinking water containing vildagliptin (10 mg·kg body wt^{-1}·day^{-1}) (39, 58), and the other groups received unsupplemented drinking water from 1 day postsurgery. The mice were allowed to drink ad libitum, and the drinking volumes were measured. The mice were fed a normal chow diet for 4 wk.

Echocardiography. Transthoracic echocardiography was performed before euthanasia as previously described (24). In brief, at 4 wk postsurgery, the mice were placed in a supine position without anesthesia. Short-axis, two-dimensional guided M-mode Doppler echocardiograms were captured and analyzed offline using a Vevo 770 High-Resolution in vivo Micro-Imaging System (VisualSonics, Toronto, Canada) equipped with a 15- to 45-MHz transducer. Left ventricular (LV) end-diastolic diameter (Dd), end-systolic diameter (Ds), and fractional shortening (FS) were measured. All measurements were made from leading edge to leading edge, according to the American Society of Echocardiography guidelines (22). Percentage FS was calculated as follows: %FS = [(LVDd − LVDs)/LVDd] × 100. The investigator performing and interpreting the echocardiograms was blinded to the subgroups.

Hemodynamic assessment. To confirm pressure overload, four to five mice in each group were randomly selected for LV pressure measurement, as previously described (27). In brief, under pentobarbital anesthesia, an endotracheal tube was inserted and connected to a volume-cycled rodent ventilator. A 1.4-Fr micromanometer-tipped catheter (Millar Instruments, Houston, TX) was inserted into the right carotid artery, blood pressure and heart rate were measured simultaneously, and data were acquired using the PowerLab Data Acquisition System (AD Instruments, Bella Vista, NSW, Australia).

Analysis of intraperitoneal glucose tolerance test. Four weeks after either TAC or sham operation, about half of the surviving mice, namely five mice in each sham-operated group and 12 and 8 mice in TAC with and without vildagliptin groups, were randomly selected for an intraperitoneal glucose tolerance test following overnight fasting (12–16 h). As overnight fasting and glucose injection might be stressful, we enrolled only half of the surviving mice to reduce the effect on additional deaths. Glucose (1 mg/kg body wt) was injected into the intraperitoneal cavity, as previously described (54). Blood was sampled from the tail prior to and at 30, 60, 90, and 120 min after glucose administration. Blood glucose concentrations were measured by a glucose meter using the glucose oxidase method (Glutest Ace R; Sanwa Kagaku Kenkyusho, Nagoya, Japan).

GLP-1 measurement [ELISA]. Four weeks after treatment, their chests were opened under anesthesia 1 h after feeding following overnight fasting for GLP-1 measurement by enzyme-linked immunosorbent assay (ELISA). Blood samples were obtained from the hearts and immediately collected in BD P700 tubes (Becton Dickinson, Franklin Lakes, NJ) containing EDTA and DPP-IV protease inhibitor cocktail. The tubes were centrifuged at 1,200 *g* for 10 min to extract plasma. The plasma samples were then stored at −80°C in a freezer until GLP-1 assay. Plasma GLP-1 levels were measured using a Glucagon-Like Peptide-1 (Active) ELISA Kit (Millipore, Billerica, MA) according to the manufacturer's instructions (52). The GLP-1 ELISA measures biologically active GLP-1-(7–37) and GLP-1-(7–36)-NH_2 but does not cross-react with glucagon, GLP-2, inactive GLP-1-(9–37) or GLP-1-(9–37)-NH_2.

Histology and immunohistochemistry. Histochemical analysis was performed as previously described (25). Briefly, the surviving mice were euthanized after 4 wk of observation. The hearts were harvested, and cardiac tissues were fixed with 4% paraformaldehyde. The fixed samples were embedded in paraffin and sectioned at 4-μm thickness for picrosirius red staining. The extent of myocardial collagen was analyzed in five hearts from each group (30). The original images were digitized and transformed into binary images, and each area was calculated using ImageJ software (NIH, Bethesda, MD). The total myocardial collagen index was defined as the total area of collagen content in the entire microscopic field divided by the total connective tissue area plus the myocardial area. The terminal deoxynucleotidyl transferase dUTP nick-end labeling (TUNEL) assay was performed using an ApopTag Peroxidase In Situ Apoptosis Detection Kit (Millipore), according to the manufacturer's instructions. The number of TUNEL-positive cells was expressed as a percentage of total cells, as previously described (35).

Real-time quantitative polymerase chain reaction. Four weeks after TAC, murine ventricles were processed for total RNA isolation using TRIzol reagent (Invitrogen, Carlsbad, CA) according to the manufacturer's instructions. First-strand cDNA was synthesized from 1 μg total RNA using the High-Capacity cDNA Reverse Transcription Kit (Applied Biosystems, Foster City, CA). The primers and probes used to quantify *transforming growth factor-1β (Tgf-1β)* and *glyceraldehyde 3-phosphate dehydrogenase (Gapdh)* were recommended by the manufacturer (Applied Biosystems). Real-time quantitative reverse transcriptase polymerase chain reaction (RT-PCR) was performed in a StepOne Real-Time PCR System (Applied Biosystems). From each amplification plot, a threshold cycle (Ct) value was calculated, representing the PCR cycle number at which fluorescence was detectable above an arbitrary threshold. Each sample was analyzed in duplicate, and the results were systematically normalized to GAPDH expression using the ΔΔCt method (29).

Western blot analysis. LV samples frozen at −80°C were placed on ice, homogenized, and lysed with lysis buffer [1% NP-40, 150 mM NaCl, 20 mM Tris pH 7.5, 2 mM EDTA, 50 mM NaF, 1 mM Na_3VO_4, plus protease inhibitor cocktail (Nacalai tesque, Kyoto, Japan)]. The supernatant was loaded onto 10%–15% sodium dodecyl sulfate-polyacrylamide gel electrophoresis gels. Immunoblotting was performed as previously described (41). The ChemiDoc XRS System (Bio-Rad Laboratories, Hercules, CA) was used for chemiluminescence imaging. Primary antibodies against phospho-Smad2 (p-Smad2), p-Smad3, caspase-3, and cleaved caspase-3 primary antibodies were purchased from Cell Signaling Technology (Beverly, MA); anti-Smad2/3 primary antibody was purchased from BD Transduction Laboratories (Franklin Lakes, NJ); and anti-GAPDH (used as a loading control) primary antibody was purchased from Millipore. Target bands were identified using ECL prime and ECL Select Western blotting reagents (GE Healthcare, Little Chalfont, Buckinghamshire, UK). Protein bands were quantified by densitometry.

Statistical analysis. All of the data are expressed as means ± SE and were analyzed by repeated-measures analysis of variance (ANOVA) followed by Bonferroni test and Student's *t*-test for paired and nonpaired data as appropriate. The differences in the number of surviving mice were analyzed by Kaplan-Meier method. P values of <0.05 were considered significant using JMP 8.0.1 software (SAS Institute, Cary, NC).

RESULTS

Hemodynamic measurements. The blood pressures and heart rates 4 wk after TAC were similar in the sham-operated groups with and without vildagliptin (71.2 ± 3.1 vs. 74.5 ± 3.2

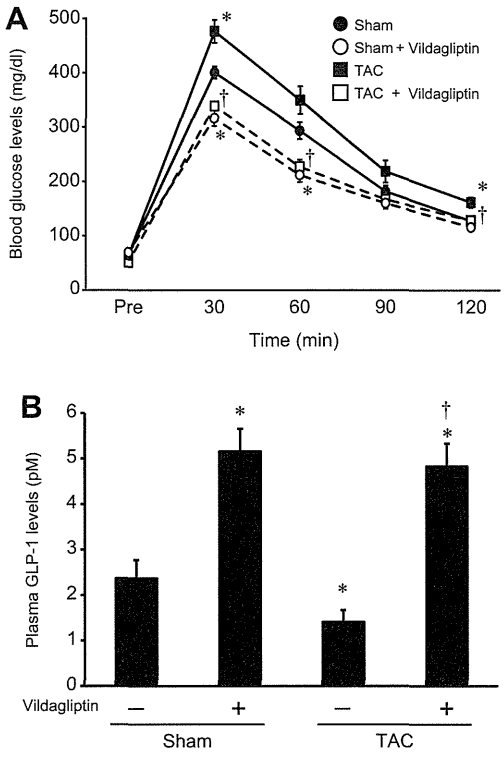

Fig. 1. *A*: plasma glucose levels measured by intraperitoneal glucose tolerance test. Sham-operated mice (n = 5), sham-operated mice with vildagliptin (n = 5), mice with transverse aortic constriction (TAC) (n = 8), and TAC mice with vildagliptin (n = 12) were enrolled. *B*: plasma levels of glucagon-like peptide-1 (GLP-1) 4 wk after TAC or sham operation. All blood samples were collected 1 h after feeding following overnight fasting. Sham-operated (n = 8), sham-operated mice with vildagliptin (n = 10), TAC mice (n = 15), and TAC mice with vildagliptin (n = 21) were measured. The data shown are means ± SE. *$P < 0.05$ vs. sham operated, †$P < 0.05$ vs. TAC.

mmHg; 459 ± 36 vs. 451 ± 22 beats/min; $P = 0.482$ and $P = 0.830$, respectively; n = 5 in each group), and in the TAC groups with and without vildagliptin (101.4 ± 9 vs. 121.4 ± 10 mmHg; 394 ± 80 vs. 463 ± 27 beats/min; $P = 0.193$ and $P = 0.400$; n = 5 and n = 4, respectively).

Intraperitoneal glucose tolerance test and plasma GLP-1 levels. Figure 1*A* shows the results of the intraperitoneal glucose tolerance test. Blood glucose levels at 30 and 120 min after intraperitoneal glucose injections were higher in the TAC mice than in the sham-operated mice (TAC vs. sham operated: 476.4 ± 20.9 vs. 400.5 ± 11.2 mg/dl at 30 min, and 161.5 ± 9.4 vs. 127.3 ± 8.3 mg/dl at 120 min, n = 8 and 5; $P < 0.05$). This was consistent with our previous report (27) in which TAC mice exhibited impaired glucose tolerance. Vildagliptin administration decreased blood glucose levels at each time point after glucose injection in TAC mice (with vs. without vildagliptin: 345.1 ± 7.9 vs. 476.4 ± 20.9 mg/dl at 30 min, 245.5 ± 13.1 vs. 349.6 ± 25.3 mg/dl at 60 min, and 127.9 ± 8.5 vs. 161.5 ± 9.4 mg/dl at 120 min, n = 12 and 8; $P < 0.05$).

We evaluated the GLP-1 levels in the TAC mice with or without vildagliptin. Because ad libitum feeding could have affected the plasma GLP-1 levels, we conducted a preliminary experiment to identify the optimal conditions for GLP-1 measurement. Nine-week-old C57BL6/J mice were fed a normal chow diet, divided into two groups, and treated with or without vildagliptin for 4 wk, as described above. To evaluate whether feeding affected the plasma GLP-1 levels, the mice were fasted 12 h before blood sampling. We randomly separated each group into two subgroups; the two subgroups were fasted further, and the others were allowed to feed 1 h before sampling. Under fasting conditions, vildagliptin produced a statistically insignificant increase in GLP-1 levels (with vs. without vildagliptin: 5.19 ± 1.04 vs. 3.93 ± 0.70 pM, n = 5 each; $P > 0.05$). In the mice sampled 1 h after feeding, GLP-1 levels were elevated with in the vildagliptin group (with vs. without vildagliptin: 9.13 ± 2.35 vs. 4.47 ± 0.87 pM, n = 4 and 5; $P < 0.05$), suggesting that this sampling time schedule, i.e., 1 h after food intake, was suitable for plasma GLP-1 measurement. Figure 1*B* shows the plasma GLP-1 levels under this time schedule. The GLP-1 levels were decreased in the TAC mice (sham operated vs. TAC: 2.37 ± 0.40 vs. 1.41 ± 0.26 pM, n = 8 and 15; $P < 0.05$), but elevated in TAC mice with vildagliptin to the levels of sham-operated mice with vildagliptin (with vs. without vildagliptin: 4.83 ± 0.50 vs. 1.41 ± 0.26 pM, n = 21 and 15; $P < 0.05$).

Echocardiography. Representative echocardiographic images are shown in Fig. 2. Echocardiographic analysis revealed enlarged Dd and Ds in the TAC mice both with and without vildagliptin (n = 27 and 17). Both LV dilatation and dysfunction in the TAC group were ameliorated by vildagliptin treatment (Fig. 3).

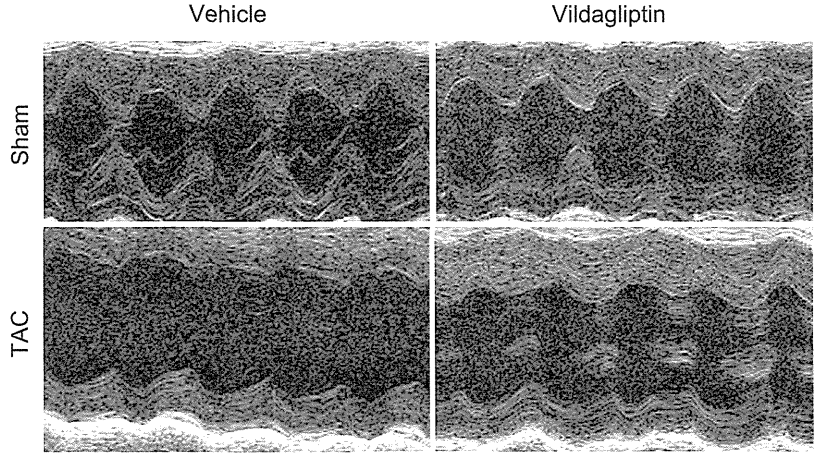

Fig. 2. Representative M-mode echocardiograms of mice 4 wk after TAC or sham operation. Top left, sham operated; top right, sham operated with vildagliptin; bottom left, TAC; bottom right, TAC with vildagliptin.

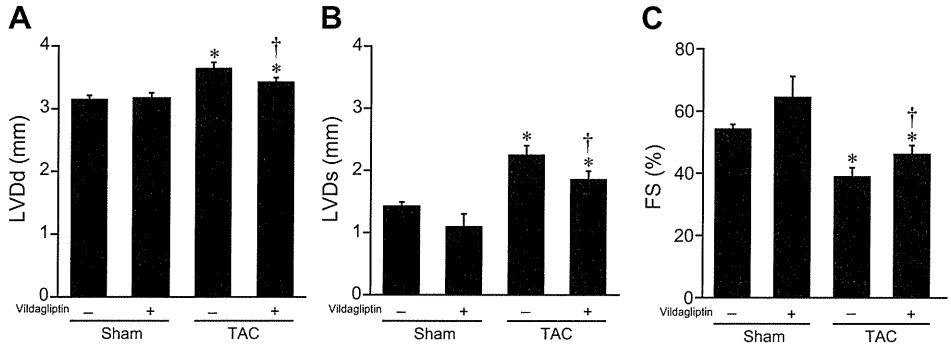

Fig. 3. *A* and *B*: left ventricular (LV) dimensions. *C*: fractional shortening (FS) 4 wk after TAC or sham operation. LV end-diastolic diameter (Dd), end-systolic diameter (Ds), and FS measured by echocardiography at 4 wk after TAC or sham operation. Echocardiographic analysis revealed enlarged LV end-diastolic and end-systolic diameters in both of the TAC groups compared with the sham-operated mice. Both LV dilatation and dysfunction in the TAC group were ameliorated by vildagliptin treatment. Sham-operated mice (n = 5), sham-operated mice with vildagliptin (n = 5), TAC mice (n = 17), and TAC mice with vildagliptin (n = 27) were examined. LVDd, LV end-diastolic dimension; LVDs, LV end-systolic dimension. Data shown are means ± SE. *$P < 0.05$ vs. sham operated, †$P < 0.05$ vs. TAC.

Water uptake and heart weight. Body weight was not statistically different between the groups: 24.3 ± 1.7 g and 23.4 ± 1.4 g in the sham-operated and TAC mice without vildagliptin (n = 10 and 17), 25.8 ± 1.7 g and 25.2 ± 2.4 g in the sham-operated and TAC mice with vildagliptin (n =10 and 27). Heart weight-to-body weight ratio (HW/BW) markedly increased in the TAC group compared with the sham-operated group (4.9 ± 0.1 vs. 9.3 ± 0.5 for sham-operated and TAC mice without vildagliptin, respectively; $P < 0.05$), and vildagliptin did not attenuate HW/BW (9.2 ± 0.4 for TAC with vildagliptin; Fig. 4). Volumes of vildagliptin solution or water consumed were similar in all of the groups (5.2 ± 0.2, 4.9 ± 0.5, 4.4 ± 0.9, and 4.5 ± 1.3 ml/day for sham-operated with and without vildagliptin and TAC with and without vildagliptin, respectively; $P \geq 0.05$ for all).

Apoptosis and fibrosis. We performed TUNEL staining to clarify the degree of apoptosis in the murine hearts. Apoptosis in the myocardium of the TAC mice was increased compared with the sham-operated mice, and this increase in apoptotic cell death was largely attenuated by vildagliptin (Fig. 5, *A* and *B*, n = 4 per each group). Next we performed immunoblotting to confirm apoptotic changes in protein levels. We observed increased cleaved caspase-3 protein in pressure-overloaded murine hearts, which was partially ameliorated by vildagliptin (Fig. 5, *C* and *D*, n = 4 per each group). These findings indicate that vildagliptin partly reduces myocardial apoptosis in pressure-overloaded murine hearts.

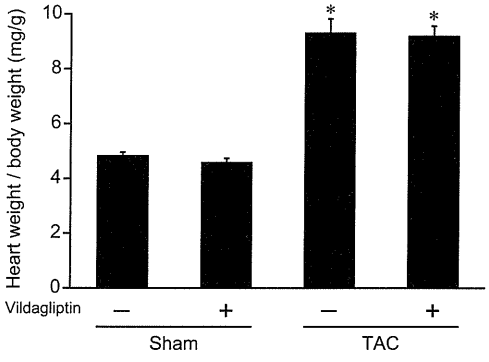

Fig. 4. Heart weight (mg)/body wt (g) ratio 4 wk after the TAC or sham operation. Sham-operated mice (n = 10), sham-operated mice with vildagliptin (n = 10), TAC mice (n = 17), and TAC mice with vildagliptin (n = 27) mice were measured. The values shown are means ± SE. *$P < 0.05$ vs. sham operated.

Figure 6*A* shows increases in myocardial collagen in the TAC group, also ameliorated by vildagliptin. Figures 6*B* shows fibrotic areas identified by picrosirius red staining. The total myocardial interstitial collagen area significantly increased in the TAC group compared with the sham-operated groups ($P <$ 0.05 vs. sham operated, n = 5 per each group) but was decreased in the TAC with vildagliptin group ($P < 0.05$ vs. TAC) (sham operated, 1.79 ± 0.22%; sham operated with vildagliptin, 1.77 ± 0.20%; TAC, 12.12 ± 0.27%; TAC with vildagliptin, 8.02 ± 1.84%). We next analyzed expression of *Tgf-1β*, a fibrosis-related gene, using RT-PCR. Myocardial *Tgf-1β* expression significantly increased in the TAC group compared with that in the sham-operated group ($P < 0.05$ vs. sham operated) but significantly decreased in the groups with vildagliptin ($P < 0.05$ vs. TAC; sham operated, 1 ± 0.08; sham operated with vildagliptin, 0.98 ± 0.11; TAC, 1.85 ± 0.12; TAC with vildagliptin, 1.55 ± 0.06; Fig. 6*C*, n = 3 per each group).

Finally, we performed immunoblotting to verify the fibrotic changes that arose through increased levels of TGF-β pathway proteins. We observed increased p-Smad2 and p-Smad3 protein levels in the pressure-overloaded murine hearts, which were partially restored by vildagliptin (Fig. 7, n = 4 per each group). These findings indicate that vildagliptin reverses myocardial fibrosis via the TGF-β pathway in murine pressure-overloaded hearts.

Survival analysis. The number of TAC mice without vildagliptin was 41 and the number of those with vildagliptin was 40. Only 17 (41.5%) TAC mice without vildagliptin survived 28 days, whereas 27 (67.5%) TAC mice with vildagliptin survived 28 days (Fig. 8; $P < 0.05$). These data indicate that vildagliptin treatment is strongly protective. Vildagliptin did not affect the survival rate in the sham-operated mice.

DISCUSSION

This study was the first to demonstrate that a DPP-IV inhibitor improved survival rate in mice with pressure-overloaded HF. We presented the following experimental evidence: *1*) TAC exacerbated the development of impaired glucose

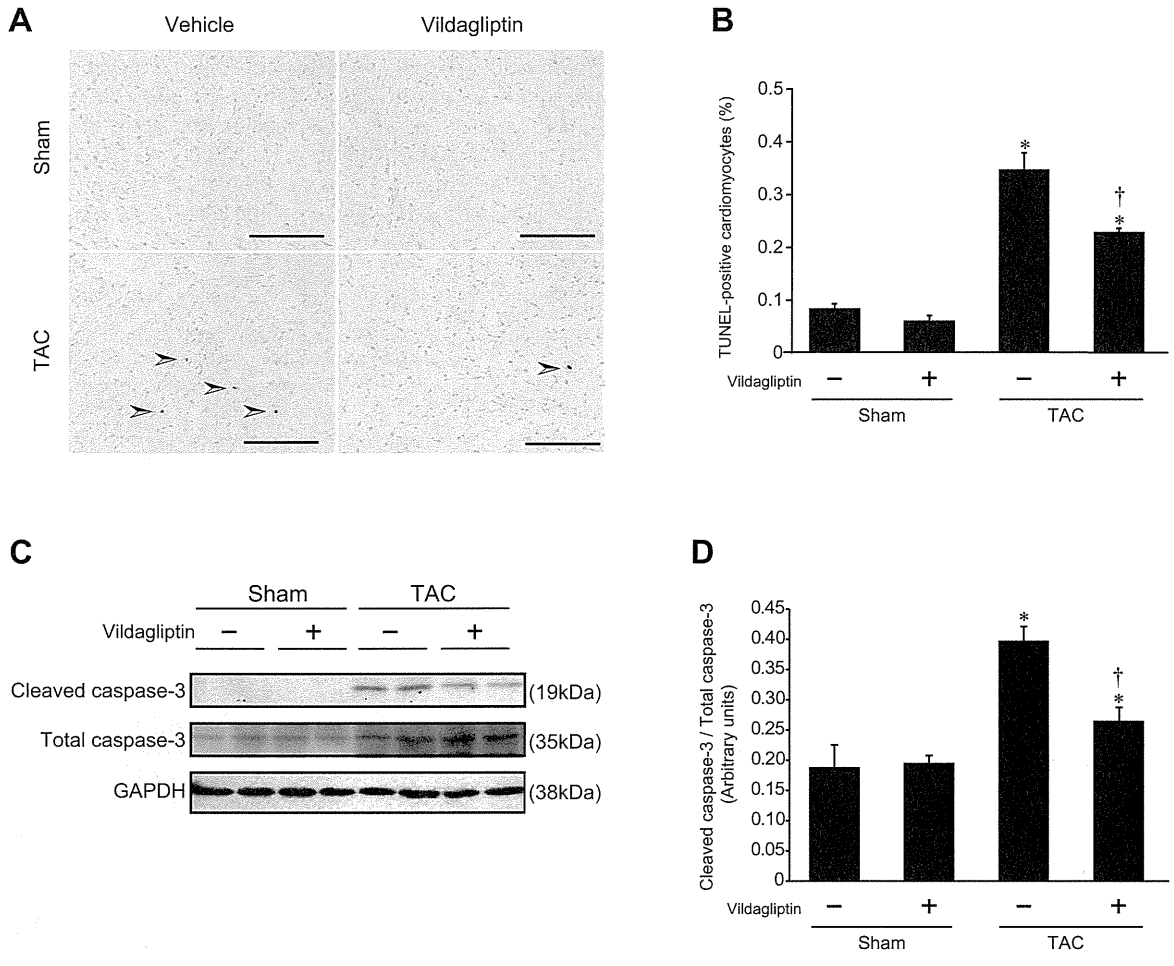

Fig. 5. *A*: representative images of the terminal deoxynucleotidyl transferase dUTP nick-end labeling (TUNEL)-positive cells in murine hearts. Top left, sham operated; top right, sham operated with vildagliptin; bottom left, TAC; bottom right, TAC with vildagliptin. Evidence of apoptosis, including chromatin condensation, is indicated with arrowheads. The proportion of TAC-induced apoptotic cells was decreased by vildagliptin. Bar = 200 μm; original magnification, ×200. *B*: quantitative analysis of murine apoptotic cardiomyocytes. TAC increased the number of apoptotic cells in the myocardium compared with the sham-operated group, and vildagliptin attenuated the increase in apoptosis. $n = 4$ for each group. *C*: representative immunoblotting analysis of cleaved/total caspase-3 and GAPDH in the hearts of sham-operated and TAC mice with or without vildagliptin. *D*: intensity of bands was quantified from four independent experiments by densitometry. Cleaved/total caspase-3 protein levels were increased by pressure overload in the hearts of TAC mice, which were reversed in TAC mice with vildagliptin. $n = 4$ for each group. The values shown are means ± SE. *$P < 0.05$ vs. sham operated, †$P < 0.05$ vs. TAC.

tolerance, which was attenuated by vildagliptin with an attendant increase in total GLP-1 levels; *2*) TAC induced myocardial apoptosis and fibrosis, which were attenuated by vildagliptin; *3*) TAC increased LVDd and LVDs, leading to FS decline, while vildagliptin attenuated increased LVDd and LVDs and increased LVFS. These effects may contribute to the improvement in survival rate generated by vildagliptin in mice with pressure overload-induced HF.

We demonstrated that TAC exacerbated the development of impaired glucose tolerance, which was attenuated by vildagliptin. This result implies that HF causes impaired glucose tolerance and improvement of impaired glucose tolerance may ameliorate HF severity. Glycemic control independently correlates with reduced LV contractile reserve and positivity for HF in diabetic patients (12, 28). We previously reported that HF is associated with impaired glucose tolerance in mice and dogs, and that correction of impaired glucose tolerance with voglibose or metformin reduces HF severity (26, 27, 41). Shimizu et al. (46) reported that systolic dysfunction induced by pressure overload exacerbates plasma glucose and hepatic insulin resistance via Akt and insulin signaling in rodents. In humans, chronic HF is associated with hyperinsulinemia (36, 51). Insulin resistance observed in HF is partly due to the lack of activity and increase in weight gain/fat redistribution. Stolen et al. (49) showed that exercise training improved insulin-stimulated myocardial glucose uptake in patients with dilated cardiomyopathy. Ashrafian et al. (2) proposed the other mechanism of HF-induced insulin resistance. Hyperadrenergic state of HF initiates the elevation of plasma free fatty acids (FFAs). The elevation of plasma FFAs induces insulin resistance due to increased triglycerides, increased cellular FFAs, and increased cytoplasmic fatty acid metabolites in hearts and skeletal muscle (43).

To our knowledge, this is the first study to evaluate an improvement in impaired glucose tolerance in animals with HF in the presence of DPP-IV inhibitors. Indeed, vildagliptin increased the plasma GLP-1 levels in animals with TAC-induced HF, suggesting that HF is attenuated by the correction

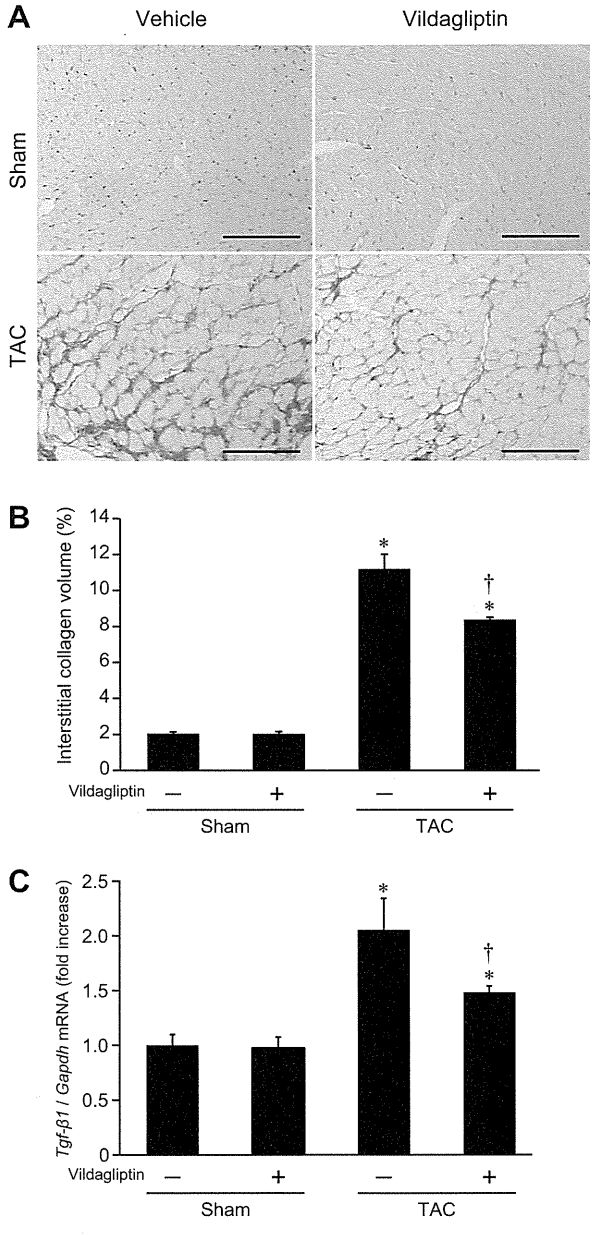

Fig. 6. *A*: representative images of the murine myocardium stained by picrosirius red. Collagen accumulation induced by TAC was regressed with vildagliptin. Top left, sham operated; top right, sham operated with vildagliptin; bottom left, TAC; bottom right, TAC with vildagliptin. Bar = 100 μm; original magnification, ×400. *B*: quantitative analysis shows that vildagliptin ameliorated myocardial collagen deposition resulting from pressure overload. $n = 5$ for each group. *C*: quantitative analysis of *transforming growth factor-1 β (Tgf1β)* in murine hearts: the expression level (normalized to *Gapdh*) in TAC group was increased compared with that in sham operated, which was alleviated in TAC with vildagliptin. $n = 3$ for each group. Data are presented as the relative change vs. sham operated. The values shown are means ± SE. *$P < 0.05$ vs. sham operated, †$P < 0.05$ vs. TAC.

of glucose intolerance by DPP-IV inhibitors. This hypothesis is supported by our findings that vildagliptin attenuates LV apoptosis and fibrosis in the TAC mice, which may explain the amelioration of LV dilatation and dysfunction. This evidence is consistent with previous studies in which sitagliptin was shown to attenuate HF severity induced by rapid pacing in pigs (14), ameliorate myocardial fibrosis in diabetic ($db/db^{-/-}$) mice (23), and improve diastolic dysfunction without altering ejection fraction in a rat model of uremic cardiomyopathy (9).

Intriguingly, GLP-1 reportedly has cardioprotective properties besides its ability to correct glucose intolerance in HF. GLP-1 receptors are expressed in the heart and activate PI3 kinase and Akt in addition to cyclic AMP (6, 19). Protein kinase A activation via accumulation of cyclic AMP may activate p38 MAP kinase, which may in turn mediate cardio-

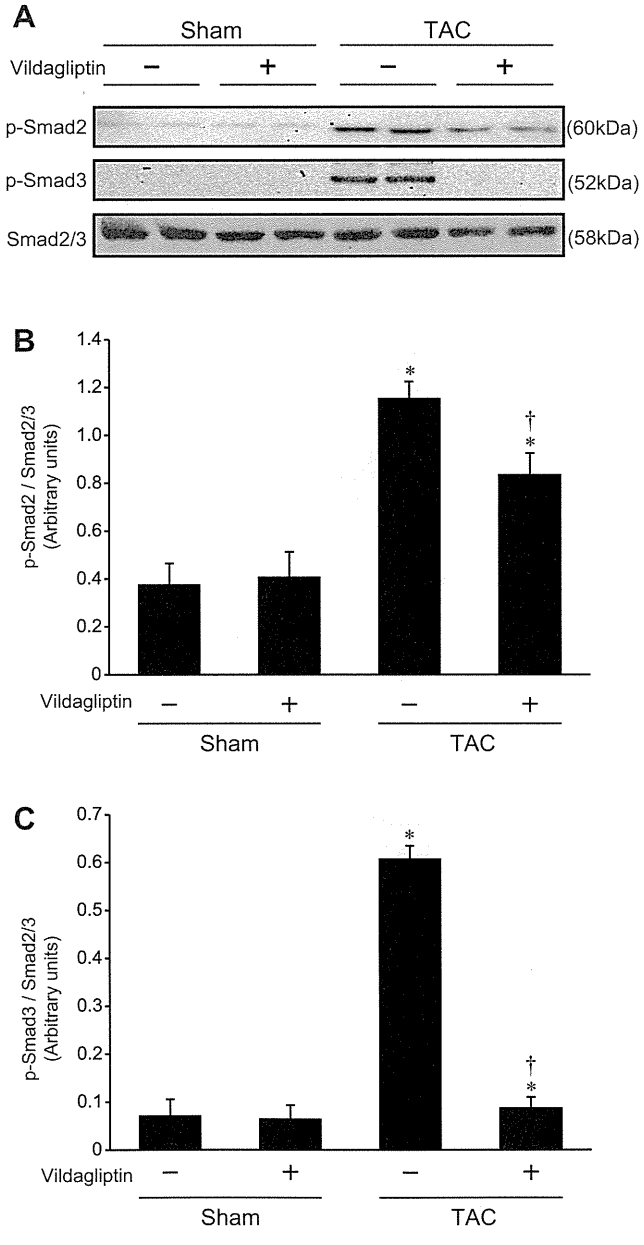

Fig. 7. *A*: representative immunoblotting analysis of phosphorylated Smad2 (p-Smad2), p-Smad3, and Smad2/3 in the hearts of sham-operated and TAC mice with or without vildagliptin. *B*: band intensity quantified by densitometry. p-Smad2/Smad2/3 protein levels increased as a result of pressure overload in the hearts of TAC mice, but recovered in TAC mice with vildagliptin. *C*: band intensity quantified by densitometry. p-Smad3/Smad2/3 protein levels increased as a result of pressure overload in the hearts of the TAC mice, but recovered in the TAC mice with vildagliptin. $n = 4$ for each group. The values shown are means ± SE. *$P < 0.05$ vs. sham operated, †$P < 0.05$ vs. TAC.

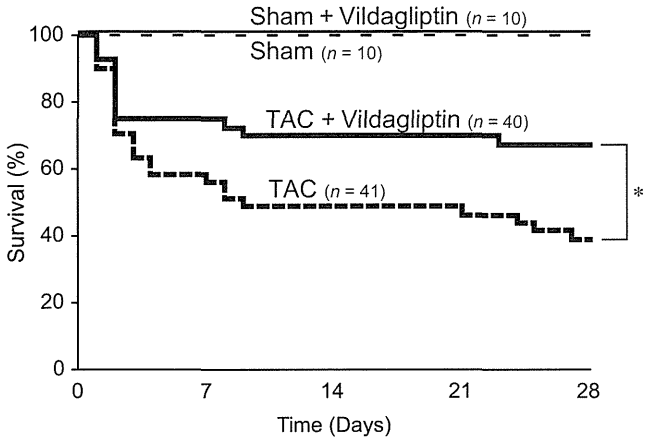

Fig. 8. The Kaplan-Meier curve analysis shows that the TAC group with vildagliptin exhibited improved survival compared with the TAC group without vildagliptin. We enrolled 41 mice in the TAC and 40 mice in the TAC with vildagliptin groups, respectively. The survival rates at 28 days after the TAC operation were 41.5% (17/41) in the TAC and 67.5% (27/40) in the TAC with vildagliptin groups, respectively. *$P < 0.05$ vs. TAC; *n*, number of mice.

protection (40, 59), and activation of PI3 kinase and Akt may further enhance these cardioprotective effects. A recent report (55) demonstrated amelioration of nonalcoholic steatohepatitis in mice by an analog of exenatide, a GLP-1 receptor agonist, supporting the antifibrotic effect of GLP-1 in murine hearts. Indeed, GLP-1 administration in patients with HF decreased the HF severity with or without DM, suggesting that GLP-1 may have cardioprotective properties independent of its effects on blood glucose levels (48). However, GLP-1 levels were elevated ~10-fold (17), significantly higher than the GLP-1 levels observed with DPP-IV inhibitors (4), suggesting that even a 1-pM increase in GLP-1 may be sufficient for cardioprotection. Moreover, in a large meta-analysis, vildagliptin was not associated with an increased risk of adjudicated cardio- and cerebrovascular events relative to all comparators in the patients with type 2 diabetes, including increased cerebrovascular risks (44). Chaykovska et al. (9) showed that increased *Tgf-β1*, *collagen type I α1*, and *collagen type III α1* expression in uremic rat hearts, compared with the sham-operated rat hearts, was significantly reduced by linagliptin, a DPP-IV inhibitor, supporting our observations. Importantly, DPP-IV inhibitors impact cardioprotection independently of GLP-1; DPP-IV also reportedly degrades peptides tyrosine-tyrosine, stromal cell-derived factor-1, and B-type natriuretic peptide (BNP) (7, 32, 45, 47). Taken together, these data suggest that DPP-IV inhibitors are cardioprotective, suggesting that they may also be beneficial for patients with HF. However, this hypothesis is limited because we used 8-wk-old mice with TAC as a model of HF in this study. Although this model is one of established animal models for HF, this model is not the universal model for the patients with HF, or does not mimic the background of the HF patients (e.g., age, dyslipidemia, ischemia, etc.). Further basic and preclinical studies are needed to apply DPP-IV inhibitors to HF patients.

The most important issue in this study was to determine whether DPP-IV inhibitors increase the survival rate because improvements in HF do not necessarily increase the survival rate. Indeed, inotropic agents such as phosphodiesterase III inhibitors (e.g., vesnarinone) improved pathophysiological parameters of HF in basic studies, even improving symptoms and cardiac function in patients with HF in clinical studies, but these drugs actually decreased the patient survival rate in large-scale clinical trials (10). This unexpected finding is attributable to the fact that the effect of these drugs on survival rate was never tested in experimental models of chronic HF. Yin et al. (60) reported the rat models with the administration of vildagliptin 2 days before or 3 wk after acute myocardial infarction surgery. They did not show the cardiac contractility and survival or any change in glucose metabolism with vildagliptin treatment. Compared with their protocol, we administered vildagliptin from 1 day postsurgery of murine TAC, which finally reversed the survival rate. These discrepancies between the study of Yin et al. and our present study may be attributable to the manner of HF induction (e.g., models and species), their glucose levels, and the dosage of vildagliptin. Their echocardiographic data seem to show worse HF than ours, which was too severe to treat with their dose set. In addition, although they did not mention any condition of the feeding (e.g., fasting or ad libitum feeding) during sampling, no difference in their blood glucose levels may suggest that the dosage was not enough to be cardioprotective. We observed that vildagliptin increased survival rate in the context of pressure overload-induced HF in mice, indicating that an adequate dose of DPP-IV inhibitors is ultimately cardioprotective against HF.

This study includes the limitations. Since TAC animals are fragile, especially when using the narrower size of needle (30 gauge) to create severe HF, the procedures of the examination such as glucose tolerance test may worsen the HF of the TAC mice. Indeed, in the preliminary study, we tried to perform oral glucose tolerance test at first, but 2 of 6 died because of the onset of acute severe HF (pulmonary edema shown by dissection). This is the reason that we shifted to the intraperitoneal glucose tolerance test, which did not cause severe HF leading to death. Importantly, the timing and number of procedures were identical in the groups with or without vildagliptin, suggesting that these additional stresses of examination to TAC do not largely affect the present results and conclusions.

In conclusion, vildagliptin, a DPP-IV inhibitor, improved the pathophysiology of HF in pressure-overloaded mice. This effect was mediated partly by improved glucose tolerance and partly by the cardioprotective effects of GLP-1, both of which ultimately improved survival following HF.

ACKNOWLEDGMENTS

We are thankful to Akiko Ogai, Chizuko Kimura, and Nobuyoshi Imai for excellent technical assistance. Vildagliptin was a gift from Novartis.

GRANTS

This work was supported by grants-in-aid from the Ministry of Health, Labor, and Welfare of Japan and the Ministry of Education, Culture, Sports, Science and Technology of Japan.

DISCLOSURES

No conflicts of interest, financial or otherwise, are declared by the author(s).

AUTHOR CONTRIBUTIONS

Author contributions: A.T., M.A., and M.K. conception and design of research; A.T., S.I., Y.Y., and Y.L. performed experiments; A.T., S.Y., and M.K. analyzed data; A.T., S.I., K.-D.M., K.S., and Y.Y. prepared figures; A.T. drafted manuscript; A.T., S.I., K.-D.M., K.S., S.S., Y.A., S.T., T.M., and H.A.

edited and revised manuscript; S.I., K.-D.M., Y.L., H.I.-U., and M.K. interpreted results of experiments; N.M. and M.K. approved final version of manuscript.

REFERENCES

1. **Abhayaratna WP, Marwick TH, Smith WT, Becker NG.** Characteristics of left ventricular diastolic dysfunction in the community: an echocardiographic survey. *Heart* 92: 1259–1264, 2006.
2. **Ashrafian H, Frenneaux MP, Opie LH.** Metabolic mechanisms in heart failure. *Circulation* 116: 434–448, 2007.
3. **Ban K, Noyan-Ashraf MH, Hoefer J, Bolz SS, Drucker DJ, Husain M.** Cardioprotective and vasodilatory actions of glucagon-like peptide 1 receptor are mediated through both glucagon-like peptide 1 receptor-dependent and -independent pathways. *Circulation* 117: 2340–2350, 2008.
4. **Bergman AJ, Stevens C, Zhou Y, Yi B, Laethem M, De Smet M, Snyder K, Hilliard D, Tanaka W, Zeng W, Tanen M, Wang AQ, Chen L, Winchell G, Davies MJ, Ramael S, Wagner JA, Herman GA.** Pharmacokinetic and pharmacodynamic properties of multiple oral doses of sitagliptin, a dipeptidyl peptidase-IV inhibitor: a double-blind, randomized, placebo-controlled study in healthy male volunteers. *Clin Ther* 28: 55–72, 2006.
5. **Bhashyam S, Fields AV, Patterson B, Testani JM, Chen L, Shen YT, Shannon RP.** Glucagon-like peptide-1 increases myocardial glucose uptake via p38alpha MAP kinase-mediated, nitric oxide-dependent mechanisms in conscious dogs with dilated cardiomyopathy. *Circ Heart Fail* 3: 512–521, 2010.
6. **Bose AK, Mocanu MM, Carr RD, Brand CL, Yellon DM.** Glucagon-like peptide 1 can directly protect the heart against ischemia/reperfusion injury. *Diabetes* 54: 146–151, 2005.
7. **Brandt I, Lambeir AM, Ketelslegers JM, Vanderheyden M, Scharpe S, De Meester I.** Dipeptidyl-peptidase IV converts intact B-type natriuretic peptide into its des-SerPro form. *Clin Chem* 52: 82–87, 2006.
8. **Bullock BP, Heller RS, Habener JF.** Tissue distribution of messenger ribonucleic acid encoding the rat glucagon-like peptide-1 receptor. *Endocrinology* 137: 2968–2978, 1996.
9. **Chaykovska L, von Websky K, Rahnenfuhrer J, Alter M, Heiden S, Fuchs H, Runge F, Klein T, Hocher B.** Effects of DPP-4 inhibitors on the heart in a rat model of uremic cardiomyopathy. *PloS One* 6: e27861, 2011.
10. **Cohn JN, Goldstein SO, Greenberg BH, Lorell BH, Bourge RC, Jaski BE, Gottlieb SO, McGrew F, 3rd DeMets DL, White BG.** A dose-dependent increase in mortality with vesnarinone among patients with severe heart failure. Vesnarinone Trial Investigators. *N Engl J Med* 339: 1810–1816, 1998.
11. **Deacon CF, Nauck MA, Toft-Nielsen M, Pridal L, Willms B, Holst JJ.** Both subcutaneously and intravenously administered glucagon-like peptide I are rapidly degraded from the NH2-terminus in type II diabetic patients and in healthy subjects. *Diabetes* 44: 1126–1131, 1995.
12. **Egstrup M, Kistorp CN, Schou M, Hofsten DE, Moller JE, Tuxen CD, Gustafsson I.** Abnormal glucose metabolism is associated with reduced left ventricular contractile reserve and exercise intolerance in patients with chronic heart failure. *Eur Heart J Cardiovasc Imaging* 14: 349–357, 2013.
13. **Falcao-Pires I, Hamdani N, Borbely A, Gavina C, Schalkwijk CG, van der Velden J, van Heerebeek L, Stienen GJ, Niessen HW, Leite-Moreira AF, Paulus WJ.** Diabetes mellitus worsens diastolic left ventricular dysfunction in aortic stenosis through altered myocardial structure and cardiomyocyte stiffness. *Circulation* 124: 1151–1159, 2011.
14. **Gomez N, Touihri K, Matheeussen V, Mendes Da Costa A, Mahmoudabady M, Mathieu M, Baerts L, Peace A, Lybaert P, Scharpe S, De Meester I, Bartunek J, Vanderheyden M, McEntee K.** Dipeptidyl peptidase IV inhibition improves cardiorenal function in overpacing-induced heart failure. *Eur J Heart Fail* 14: 14–21, 2012.
15. **Greig NH, Holloway HW, De Ore KA, Jani D, Wang Y, Zhou J, Garant MJ, Egan JM.** Once daily injection of exendin-4 to diabetic mice achieves long-term beneficial effects on blood glucose concentrations. *Diabetologia* 42: 45–50, 1999.
16. **Gutzwiller JP, Drewe J, Goke B, Schmidt H, Rohrer B, Lareida J, Beglinger C.** Glucagon-like peptide-1 promotes satiety and reduces food intake in patients with diabetes mellitus type 2. *Am J Physiol Regul Integr Comp Physiol* 276: R1541–R1544, 1999.
17. **Halbirk M, Norrelund H, Moller N, Holst JJ, Schmitz O, Nielsen R, Nielsen-Kudsk JE, Nielsen SS, Nielsen TT, Eiskjaer H, Botker HE, Wiggers H.** Cardiovascular and metabolic effects of 48-h glucagon-like peptide-1 infusion in compensated chronic patients with heart failure. *Am J Physiol Heart Circ Physiol* 298: H1096–H1102, 2010.
18. **Hui H, Farilla L, Merkel P, Perfetti R.** The short half-life of glucagon-like peptide-1 in plasma does not reflect its long-lasting beneficial effects. *Eur J Endocrinol* 146: 863–869, 2002.
19. **Hui H, Nourparvar A, Zhao X, Perfetti R.** Glucagon-like peptide-1 inhibits apoptosis of insulin-secreting cells via a cyclic 5′-adenosine monophosphate-dependent protein kinase A- and a phosphatidylinositol 3-kinase-dependent pathway. *Endocrinology* 144: 1444–1455, 2003.
20. **Kane GC, Karon BL, Mahoney DW, Redfield MM, Roger VL, Burnett JC Jr, Jacobsen SJ, Rodeheffer RJ.** Progression of left ventricular diastolic dysfunction and risk of heart failure. *JAMA* 306: 856–863, 2011.
21. **Kim J, Nakatani S, Hashimura K, Komamura K, Kanzaki H, Asakura M, Asanuma H, Kokubo Y, Tomoike H, Kitakaze M.** Abnormal glucose tolerance contributes to the progression of chronic heart failure in patients with dilated cardiomyopathy. *Hypertens Res* 29: 775–782, 2006.
22. **Lang RM, Bierig M, Devereux RB, Flachskampf FA, Foster E, Pellikka PA, Picard MH, Roman MJ, Seward J, Shanewise JS, Solomon SD, Spencer KT, Sutton MS, Stewart WJ.** Recommendations for chamber quantification: a report from the American Society of Echocardiography's Guidelines and Standards Committee and the Chamber Quantification Writing Group, developed in conjunction with the European Association of Echocardiography, a branch of the European Society of Cardiology. *J Am Soc Echocardiogr* 18: 1440–1463, 2005.
23. **Lenski M, Kazakov A, Marx N, Bohm M, Laufs U.** Effects of DPP-4 inhibition on cardiac metabolism and function in mice. *J Mol Cell Cardiol* 51: 906–918, 2011.
24. **Liao Y, Ishikura F, Beppu S, Asakura M, Takashima S, Asanuma H, Sanada S, Kim J, Ogita H, Kuzuya T, Node K, Kitakaze M, Hori M.** Echocardiographic assessment of LV hypertrophy and function in aortic-banded mice: necropsy validation. *Am J Physiol Heart Circ Physiol* 282: H1703–H1708, 2002.
25. **Liao Y, Takashima S, Asano Y, Asakura M, Ogai A, Shintani Y, Minamino T, Asanuma H, Sanada S, Kim J, Ogita H, Tomoike H, Hori M, Kitakaze M.** Activation of adenosine A1 receptor attenuates cardiac hypertrophy and prevents heart failure in murine left ventricular pressure-overload model. *Circ Res* 93: 759–766, 2003.
26. **Liao Y, Takashima S, Maeda N, Ouchi N, Komamura K, Shimomura I, Hori M, Matsuzawa Y, Funahashi T, Kitakaze M.** Exacerbation of heart failure in adiponectin-deficient mice due to impaired regulation of AMPK and glucose metabolism. *Cardiovasc Res* 67: 705–713, 2005.
27. **Liao Y, Takashima S, Zhao H, Asano Y, Shintani Y, Minamino T, Kim J, Fujita M, Hori M, Kitakaze M.** Control of plasma glucose with alpha-glucosidase inhibitor attenuates oxidative stress and slows the progression of heart failure in mice. *Cardiovasc Res* 70: 107–116, 2006.
28. **Lind M, Bounias I, Olsson M, Gudbjornsdottir S, Svensson AM, Rosengren A.** Glycaemic control and incidence of heart failure in 20,985 patients with type 1 diabetes: an observational study. *Lancet* 378: 140–146, 2011.
29. **Livak KJ, Schmittgen TD.** Analysis of relative gene expression data using real-time quantitative PCR and the 2[−Delta Delta C(T)] method. *Methods* 25: 402–408, 2001.
30. **Lucas JA, Zhang Y, Li P, Gong K, Miller AP, Hassan E, Hage F, Xing D, Wells B, Oparil S, Chen YF.** Inhibition of transforming growth factor-beta signaling induces left ventricular dilation and dysfunction in the pressure-overloaded heart. *Am J Physiol Heart Circ Physiol* 298: H424–H432, 2010.
31. **Mariappan N, Elks CM, Sriramula S, Guggilam A, Liu Z, Borkhsenious O, Francis J.** NF-kappaB-induced oxidative stress contributes to mitochondrial and cardiac dysfunction in type II diabetes. *Cardiovasc Res* 85: 473–483, 2010.
32. **Mentlein R, Dahms P, Grandt D, Kruger R.** Proteolytic processing of neuropeptide Y and peptide YY by dipeptidyl peptidase IV. *Regul Pept* 49: 133–144, 1993.
33. **Nikolaidis LA, Doverspike A, Hentosz T, Zourelias L, Shen YT, Elahi D, Shannon RP.** Glucagon-like peptide-1 limits myocardial stunning following brief coronary occlusion and reperfusion in conscious canines. *J Pharmacol Exper Ther* 312: 303–308, 2005.
34. **Nikolaidis LA, Elahi D, Hentosz T, Doverspike A, Huerbin R, Zourelias L, Stolarski C, Shen YT, Shannon RP.** Recombinant glucagon-like peptide-1 increases myocardial glucose uptake and improves left ventricular performance in conscious dogs with pacing-induced dilated cardiomyopathy. *Circulation* 110: 955–961, 2004.

35. **Okada K, Minamino T, Tsukamoto Y, Liao Y, Tsukamoto O, Takashima S, Hirata A, Fujita M, Nagamachi Y, Nakatani T, Yutani C, Ozawa K, Ogawa S, Tomoike H, Hori M, Kitakaze M.** Prolonged endoplasmic reticulum stress in hypertrophic and failing heart after aortic constriction: possible contribution of endoplasmic reticulum stress to cardiac myocyte apoptosis. *Circulation* 110: 705–712, 2004.
36. **Paolisso G, Tagliamonte MR, Rizzo MR, Gambardella A, Gualdiero P, Lama D, Varricchio G, Gentile S, Varricchio M.** Prognostic importance of insulin-mediated glucose uptake in aged patients with congestive heart failure secondary to mitral and/or aortic valve disease. *Am J Cardiol* 83: 1338–1344, 1999.
37. **Redfield MM, Jacobsen SJ, Burnett JC Jr, Mahoney DW, Bailey KR, Rodeheffer RJ.** Burden of systolic and diastolic ventricular dysfunction in the community: appreciating the scope of the heart failure epidemic. *JAMA* 289: 194–202, 2003.
38. **Rijzewijk LJ, van der Meer RW, Lamb HJ, de Jong HW, Lubberink M, Romijn JA, Bax JJ, de Roos A, Twisk JW, Heine RJ, Lammertsma AA, Smit JW, Diamant M.** Altered myocardial substrate metabolism and decreased diastolic function in nonischemic human diabetic cardiomyopathy: studies with cardiac positron emission tomography and magnetic resonance imaging. *J Am Coll Cardiol* 54: 1524–1532, 2009.
39. **Roy S, Khanna V, Mittra S, Dhar A, Singh S, Mahajan DC, Priyadarsiny P, Davis JA, Sattigeri J, Saini KS, Bansal VS.** Combination of dipeptidylpeptidase IV inhibitor and low dose thiazolidinedione: preclinical efficacy and safety in *db/db* mice. *Life Sci* 81: 72–79, 2007.
40. **Sanada S, Kitakaze M, Papst PJ, Asanuma H, Node K, Takashima S, Asakura M, Ogita H, Liao Y, Sakata Y, Ogai A, Fukushima T, Yamada J, Shinozaki Y, Kuzuya T, Mori H, Terada N, Hori M.** Cardioprotective effect afforded by transient exposure to phosphodiesterase III inhibitors: the role of protein kinase A and p38 mitogen-activated protein kinase. *Circulation* 104: 705–710, 2001.
41. **Sasaki H, Asanuma H, Fujita M, Takahama H, Wakeno M, Ito S, Ogai A, Asakura M, Kim J, Minamino T, Takashima S, Sanada S, Sugimachi M, Komamura K, Mochizuki N, Kitakaze M.** Metformin prevents progression of heart failure in dogs: role of AMP-activated protein kinase. *Circulation* 119: 2568–2577, 2009.
42. **Sauve M, Ban K, Momen MA, Zhou YQ, Henkelman RM, Husain M, Drucker DJ.** Genetic deletion or pharmacological inhibition of dipeptidyl peptidase-4 improves cardiovascular outcomes after myocardial infarction in mice. *Diabetes* 59: 1063–1073, 2010.
43. **Savage DB, Petersen KF, Shulman GI.** Mechanisms of insulin resistance in humans and possible links with inflammation. *Hypertension* 45: 828–833, 2005.
44. **Schweizer A, Dejager S, Foley JE, Couturier A, Ligueros-Saylan M, Kothny W.** Assessing the cardio-cerebrovascular safety of vildagliptin: meta-analysis of adjudicated events from a large Phase III type 2 diabetes population. *Diabetes Obesity Metab* 12: 485–494, 2010.
45. **Shigeta T, Aoyama M, Bando YK, Monji A, Mitsui T, Takatsu M, Cheng XW, Okumura T, Hirashiki A, Nagata K, Murohara T.** Dipeptidyl peptidase-4 modulates left ventricular dysfunction in chronic heart failure via angiogenesis-dependent and -independent actions. *Circulation* 126: 1838–1851, 2012.
46. **Shimizu I, Minamino T, Toko H, Okada S, Ikeda H, Yasuda N, Tateno K, Moriya J, Yokoyama M, Nojima A, Koh GY, Akazawa H, Shiojima I, Kahn CR, Abel ED, Komuro I.** Excessive cardiac insulin signaling exacerbates systolic dysfunction induced by pressure overload in rodents. *J Clin Invest* 120: 1506–1514, 2010.
47. **Shioda T, Kato H, Ohnishi Y, Tashiro K, Ikegawa M, Nakayama EE, Hu H, Kato A, Sakai Y, Liu H, Honjo T, Nomoto A, Iwamoto A, Morimoto C, Nagai Y.** Anti-HIV-1 and chemotactic activities of human stromal cell-derived factor 1alpha (SDF-1alpha) and SDF-1beta are abolished by CD26/dipeptidyl peptidase IV-mediated cleavage. *Proc Natl Acad Sci USA* 95: 6331–6336, 1998.
48. **Sokos GG, Nikolaidis LA, Mankad S, Elahi D, Shannon RP.** Glucagon-like peptide-1 infusion improves left ventricular ejection fraction and functional status in patients with chronic heart failure. *J Card Fail* 12: 694–699, 2006.
49. **Stolen KQ, Kemppainen J, Kalliokoski KK, Luotolahti M, Viljanen T, Nuutila P, Knuuti J.** Exercise training improves insulin-stimulated myocardial glucose uptake in patients with dilated cardiomyopathy. *J Nucl Cardiol* 10: 447–455, 2003.
50. **Suskin N, McKelvie RS, Burns RJ, Latini R, Pericak D, Probstfield J, Rouleau JL, Sigouin C, Solymoss CB, Tsuyuki R, White M, Yusuf S.** Glucose and insulin abnormalities relate to functional capacity in patients with congestive heart failure. *Eur Heart J* 21: 1368–1375, 2000.
51. **Swan JW, Anker SD, Walton C, Godsland IF, Clark AL, Leyva F, Stevenson JC, Coats AJ.** Insulin resistance in chronic heart failure: relation to severity and etiology of heart failure. *J Am Coll Cardiol* 30: 527–532, 1997.
52. **Szeto IM, Aziz A, Das PJ, Taha AY, Okubo N, Reza-Lopez S, Giacca A, Anderson GH.** High multivitamin intake by Wistar rats during pregnancy results in increased food intake and components of the metabolic syndrome in male offspring. *Am J Physiol Regul Integr Comp Physiol* 295: R575–R582, 2008.
53. **Thrainsdottir IS, Aspelund T, Thorgeirsson G, Gudnason V, Hardarson T, Malmberg K, Sigurdsson G, Ryden L.** The association between glucose abnormalities and heart failure in the population-based Reykjavik study. *Diabetes Care* 28: 612–616, 2005.
54. **Toye AA, Lippiat JD, Proks P, Shimomura K, Bentley L, Hugill A, Mijat V, Goldsworthy M, Moir L, Haynes A, Quarterman J, Freeman HC, Ashcroft FM, Cox RD.** A genetic and physiological study of impaired glucose homeostasis control in C57BL/6J mice. *Diabetologia* 48: 675–686, 2005.
55. **Trevaskis JL, Griffin PS, Wittmer C, Neuschwander-Tetri BA, Brunt EM, Dolman CS, Erickson MR, Napora J, Parkes DG, Roth JD.** Glucagon-like peptide-1 receptor agonism improves metabolic, biochemical, and histopathological indices of nonalcoholic steatohepatitis in mice. *Am J Physiol Gastrointest Liver Physiol* 302: G762–G772, 2012.
56. **Vasan RS, Larson MG, Benjamin EJ, Evans JC, Reiss CK, Levy D.** Congestive heart failure in subjects with normal versus reduced left ventricular ejection fraction: prevalence and mortality in a population-based cohort. *J Am Coll Cardiol* 33: 1948–1955, 1999.
57. **Wei Y, Mojsov S.** Tissue-specific expression of the human receptor for glucagon-like peptide-I: brain, heart and pancreatic forms have the same deduced amino acid sequences. *FEBS Lett* 358: 219–224, 1995.
58. **Winzell MS, Ahren B.** The high-fat diet-fed mouse: a model for studying mechanisms and treatment of impaired glucose tolerance and type 2 diabetes. *Diabetes* 53, *Suppl* 3: S215–S219, 2004.
59. **Ye Y, Keyes KT, Zhang C, Perez-Polo JR, Lin Y, Birnbaum Y.** The myocardial infarct size-limiting effect of sitagliptin is PKA-dependent, whereas the protective effect of pioglitazone is partially dependent on PKA. *Am J Physiol Heart Circ Physiol* 298: H1454–H1465, 2010.
60. **Yin M, Sillje HH, Meissner M, van Gilst WH, de Boer RA.** Early and late effects of the DPP-4 inhibitor vildagliptin in a rat model of post-myocardial infarction heart failure. *Cardiovasc Diabetol* 10: 85, 2011.